SELF-TUNING FUZZY CONTROLLER FOR AIR-CONDITIONING SYSTEMS

BY

ZHENG XIAOQING

(B. Eng., M. Eng. XJTU)

A THESIS SUBMITTED

FOR THE DEGREE OF MASTER OF ENGINEERING

DEPARTMENT OF MECHANICAL ENGINEERING

NATIONAL UNIVERSITY OF SINGAPORE

2002

ACKNOWLEDGEMENTS

First and foremost, I would like to express my sincere gratitude to my supervisors, Professor Poo Aun Neow and Associate Professor Chou Siaw Kiang, for their patient guidance throughout this project. They provided me with not only technical guidance and much constructive advice on my research, but also strong encouragement and kind affection.

I would also like to thank Mr. Sacadevan Raghavan from the Air-Conditioning Laboratory in the Mechanical Engineering Department for his invaluable assistance in the experiments as well as his friendliness and eagerness to help. Many thanks also go to Mr. Duan Kaibo and Mr. Xi Xuecheng for their invaluable advice during the project. Last but by no means least, I am grateful to all colleagues for the support they give.

TABLE OF CONTENTS

SUMMARY

The simultaneous control of space temperature and humidity is required in some industrial applications. Conventionally, the accurate control is accomplished by cooling the air to the required humidity and reheating it to the required temperature subsequently. This method results in greater energy consumption. This research is aimed to realize a better way for the simultaneous control of the space temperature and relative humidity in chilled water air-conditioning systems.

In chilled water air-conditioning systems, the temperature and humidity of the supply air change with the chilled water flow rate and the supply airflow rate. A higher supply airflow rate results in a greater sensible cooling capacity but a smaller latent cooling capacity. While both the sensible cooling capacity and latent cooling capacity increase with a higher chilled water flow rate, in typical air-conditioning systems, the change in cooling capacity due to a percentage change in the supply airflow rate is greater than that due to the same percentage change in the chilled water flow rate. Because the system sensible heat load is generally greater than the latent heat load, the control strategy to control room temperature by varying the supply airflow rate and to control room relative humidity by varying the chilled water flow rate was successfully implemented in experiments. On the other hand, the other strategy of controlling the room temperature by varying the chilled water flow rate and room relative humidity by varying the supply airflow rate failed in experiments.

Fuzzy logic was used to design the control system to resolve the difficulty of developing an accurate dynamic model of the air-conditioning system. The fuzzy

controller consisted of two separate sub-controllers, a fuzzy temperature controller and a fuzzy relative humidity controller. It is shown in experiments that the designed controller was able to track the set points of room temperature and relative humidity. The fuzzy controller was insensitive to the coupling between space temperature and relative humidity. Experimental results also demonstrated the favorable disturbance rejection ability of the fuzzy controller. It was found from experiments that the values of parameters used in the fuzzy controller affect the performance of the system, including membership functions, scaling factors of input variables, output variable gains and fuzzy control rules.

Fuzzy neural networks, which integrate the advantages of fuzzy logic and neural networks, were used to resolve the time-consuming and difficult task of tuning of the fuzzy controller. Two neural networks were used in the control system which has a model reference adaptive control structure. A neural network emulator was designed to emulate the air-conditioning system. This emulator can accurately predict the response of the air-conditioning system after proper training. The other neural network, a fuzzy neural network controller, provided control signals to the air-conditioning plant. The fuzzy controller was tuned through the neural network which adjusts its weights through training using measured input-output data. The performance of the control system was investigated in actual experiments. It was found that the controller performed very well using the membership functions and fuzzy rules adjusted through training.

NOMENCLATURE

C_a	Overall thermal capacitance of air-handling unit
C_r	Room air thermal capacity
c_a	Specific heat of air
c_w	Specific heat of chilled water
d_j	Desired response of the jth output node
e_θ	Room temperature error
$\dot{e}_\theta$	Room temperature error rate
e_ϕ	Relative humidity error
$\dot{e}_\phi$	Relative humidity error rate
f_c	Chilled water flow rate
f_s	Supply airflow rate
h	Specific enthalpy
J	Objective function
K	Scaling factor
m_a	Supply air mass flow rate
m_w	Chilled water mass flow rate
m_{gain}	Moisture gain
net_j^l	Net input to the jth node in layer l
n_v	Ventilation air change
q_{plant}	Energy input from plant
q_{gain}	Room sensible heat gain
T_{set}	Settling time
T_θ	Temperature sampling period
T_ϕ	Relative humidity sampling period
U_a	Cooling coil air-side heat transfer coefficient
U_w	Cooling coil water-side heat transfer coefficient

u_f	Supply fan speed
u_v	Three-way valve opening
V_a	Volume of air-handling unit
V_r	Room volume
W_o	External humidity ratio
W_r	Room humidity ratio
W_s	Supply air humidity ratio
w_{ji}^l	Weight connecting the ith node in layer $l-1$ to the jth node in layer l
y_j^l	Output of the jth node in layer l
α_a	Overall transmittance-area factor outside air-handling unit
θ_c	Chilled water temperature
θ_{cl}	Cooling coil surface temperature
θ_d	Desired room temperature
θ_{dp}	Dew point temperature
$\overline{\theta}_f$	Surface temperature of the room fabric
θ_o	External temperature
θ_r	Room air temperature
θ_s	Supply air temperature
θ_{set}	Room temperature set point
ϕ_d	Desired room relative humidity
ϕ_r	Room relative humidity
ϕ_s	Supply air relative humidity
ϕ_{set}	Room relative humidity set point
ρ_a	Density of air
ρ_w	Density of chilled water
μ	Membership degree
η	Learning rate
δ_j^l	Local gradient for jth node in layer l

LIST OF FIGURES

LIST OF TABLES

CHAPTER 1
INTRODUCTION

The air-conditioning plant is designed to produce a conducive atmospheric environment for human beings or a special environment for some industrial and scientific processes. Temperature, humidity, air motion, and air purity within a space are controlled with an air-conditioning system. According to their applications, air-conditioning systems are usually classified into two categories: comfort air-conditioning and industrial air-conditioning.

The indoor air quality of an enclosed space has a significant effect on the health and productivity of its occupants since a person may spend much time indoors. The comfort air-conditioning system is employed to produce a comfortable environment for people. Researches over many years have identified the major factors contributing to the human thermal comfort: temperature, relative humidity, air movement, and radiant effects, among which temperature and relative humidity are generally controlled. Because man is more sensitive to temperature than to humidity, most of the comfort air-conditioning systems are designed to provide relatively accurate temperature control while keeping the relative humidity floating within some larger range, which is usually defined from 30% to 60% (ASHRAE Standard 55-1981).

Some industrial and scientific processes require simultaneous and accurate control of temperature and humidity. An example is in textile and paper processing using high-speed machinery that requires accurate control of both temperature and relative

humidity (Krakow et al., 1995a). Some scientific experiments can only be performed properly only under some specific environments. Industrial air-conditioning systems are designed for such applications.

The increasing demand for air-conditioning systems has resulted in greatly increased energy consumption. The energy consumed by heating, ventilating, air-conditioning (HVAC) equipment in industrial and commercial buildings constitutes 50% of the world energy consumption (Betzaida and Miguel, 1999). It is estimated that in Singapore, commercial buildings account for about 30% of the total electrical energy consumed in the country. Of this about 50% to 60% is consumed by air-conditioning and mechanical ventilation (ACMV) systems (Ibrahim, 1998). Energy resources are limited in supply and are ever increasing in price and therefore it is essential to find ways to improve the efficiency of systems.

1.1 Background

The variable air volume (VAV) concept was introduced due to the energy crisis in the 1970s for the purpose of energy saving. Since then, many VAV components, such as terminals, fans, air-regulating devices, and controls have been developed. The increasing applications of direct digital control (DDC) also intensify the uses of VAV technology. Variable speed drive (VSD) technology especially shows the advantage of VAV systems.

The constant air volume (CAV) systems maintain a constant quantity of supply air, and the system cooling capacity is modified through varying the supply air temperature. The chilled water flow rate is controlled to get the desired supply air temperature. In such systems, fan speed is fixed at a high speed in order to cater to the peak load.

However, the system actually operates at part load for most of the time. Thus, a large amount of energy is wasted since the energy consumption of the fan is approximately proportional to the cubic of its speed. It is also observed, in part-load conditions, that the use of a constant volume of air irrespective of the load leads to high space relative humidity.

On the other hand, a VAV system varies the supply airflow rate to a particular space based on requirements. The VAV boxes respond to the signals from room thermostats. The supply air temperature is maintained at some constant value by a discharge temperature control system, and the room temperature is controlled by varying the supply airflow rate to the space. Therefore, smaller amounts of air are used at part loads. A variable speed drive can be used for this task. Energy savings are achieved and the high relative humidity is not experienced at part-load conditions by the use of this type of systems.

As mentioned previously, it is desirable to control both space temperature and relative humidity independently and accurately in some industrial applications. These two variables, amongst others influence the rate of chemical and biochemical reactions, the rate of crystallization, density of chemical solutions, the corrosion of metals and the generation of static electricity (ASHRAE Handbook, 1999). High quality semiconductors can only be manufactured in clean rooms, for example, where the room temperature, humidity and air cleanliness are strictly controlled.

Central chilled water systems are often used in large-scale air-conditioning projects. The chilled water is produced in the central plant and flows through the air-handling

unit (AHU), where it absorbs sensible and latent heat from the passing air. The air is cooled and dehumidified after the heat transfer.

Conventionally, the accurate control of temperature and relative humidity of the conditioned space is accomplished by cooling the air to the required specific humidity and reheating it to the desirable temperature. Undoubtedly, this method increases the energy consumption. According to heat transfer theories, the chilled water flow rate and the supply airflow rate decide the system cooling capacity jointly. Variations in the supply airflow rate result in simultaneously varying supply air temperature and humidity, which can also be changed by varying the chilled water flow rate.

The behavior of the controller has direct effect on the performance of the air-conditioning system. The objective of the control system is to adjust the plant cooling capacity to adapt to the varying heat load. PID controllers are by far the most widely used and have proven themselves to be valuable and reliable in HVAC applications (Rosandich, 1997). However, PID control works most favorably on the assumption that the system model parameters do not change much. When a well-tuned PID controller is applied to another system with different model parameters, or when system parameters change during operation, its performance degrades (Kasahara et al., 1999).

In the past decades, some adaptive and self-tuning controls have been proposed with developments in modern control and stability theories (Astrom and Wittenmark, 1989; Narendra et al., 1999). In most cases, self-tuning controllers can satisfactorily replace conventional single-input single-output (SISO) PID controllers within a multi-loop

control scheme. However, although self-tuning control is capable of offering better dynamic performance than the conventional fixed gain control, it suffers from the major drawback of requiring model identification in real time.

Artificial intelligence, such as expert systems, fuzzy logic and artificial neural networks (ANNs), has been introduced to this field. The origin of artificial intelligence (AI) can be traced back to the 1950s. There is no unique definition of intelligence, the most commonly accepted definition is "intelligence is the ability to perceive, understand and learn about new situations" (Beardon, 1989). These techniques show some advantages over the conventional controls. In the present project, fuzzy logic and neural networks are investigated for their use in the control of air-conditioning systems.

Fuzzy systems allow users to give inputs in imprecise terms and use them to generate either fuzzy or precise advice. It is tolerant of model uncertainty and to the imprecision inherent in normal human thinking with the use of linguistic variables with membership functions. Artificial neural networks are distributed processing systems that have been inspired by the biological nerve system. They do not require any assumption between the input variables and the corresponding outputs. Instead, they are able to learn and build their own non-linear model from a known or measured relationship between the input and output variables during a training process. Thus, high human expertise is not needed and the difficulty of modeling is not encountered.

Fuzzy logic and neural networks have several characteristics in common. However, each has its own advantages. The advantages of fuzzy logic over neural networks are its tolerance for imprecision and explicit knowledge representation. On the other hand,

the neural networks offer other advantages such as the ability to learn from examples and to generalize from these. It is believed that the combination of fuzzy logic and neural networks can leverage the advantages of these two individual techniques.

1.2 Objectives and Scope

This project studied the simultaneous control of the temperature and relative humidity in the conditioned space. The strategy of controlling space temperature and relative humidity by varying the supply airflow rate and the chilled water flow rate was investigated. The system energy efficiency was improved because the fan need not always run at its maximum speed and reheat of the air is not needed.

Fuzzy logic was utilized to design the controller to avoid the difficulty of building a mathematical model for the air-conditioning system. In order to resolve the laborious work involved in tuning of the controller, a self-tuning fuzzy controller was proposed. A neural network was integrated with the fuzzy logic controller. This controller structure merged the individual advantages of neural networks and fuzzy logic. The model reference control scheme was used to build the control system. In the control scheme, a neural network was used to construct the fuzzy logic controller and parameters in the fuzzy controller were treated as the connecting weights in the network. In this way, tuning of the fuzzy controller was achieved by training of the neural network.

The air-conditioning system for the project was a chilled water system for a thermal chamber in the Mechanical Engineering Department, National University of Singapore. Two three-way valves were used to modify the chilled water flow rate and one variable speed fan was installed in the air-handling unit. System data such as the supply air

temperature and relative humidity, room temperature and relative humidity, three-way valve position, and supply air fan speed were recorded in experiments.

The feasibility of the control strategy was confirmed by both theoretical analyses and experimental results. The designed control system was implemented and applied to the thermal chamber to study its performance.

1.3 Outline of Thesis

This thesis is divided into six chapters. Chapter 1 gives the background, objectives and scope, and outline of the thesis. Chapter 2 reviews previous literatures on temperature and relative humidity control of air-conditioning systems. An overview of fuzzy logic and neural networks is also given in this chapter. The modeling of air-conditioning systems and their main components is done in Chapter 3. Although an accurate system model is not derived or determined as this is not necessary for the proposed controller, the general behavior and relationships between the input and output parameters are discussed as these are required for the proper design of the controller. The system modeling shows the feasibility of the control strategy. Chapter 4 describes the design of the fuzzy logic controller and the results of experiments conducted to investigate its performance. The fuzzy neural network controller is presented in Chapter 5. The conclusions are given in Chapter 6 as well as some recommendations for future developments.

CHAPTER 2
LITERATURE REVIEW

2.1 Temperature and Humidity in the Conditioned Spaces

Temperature and relative humidity (RH) are among the most important thermodynamic variables in commercial and industrial air-conditioning and in process control. These two variables, amongst others, influence the rate of chemical and biochemical reactions, the rate of crystallization and the density of chemical solutions, the corrosion of metals, the generation of static electricity, the manufacturing of printed circuit boards in test chambers, and human comfort (ASHRAE, 1995). The space temperature is dependent on the sensible heat load and system sensible cooling capacity, while the RH is dependent on the latent heat load and system latent cooling capacity. In order to accomplish the simultaneous control of temperature and RH, the air-conditioning systems must be designed to cater to both sensible and latent components of the heat load.

The lower humidity may be obtained by mechanical and chemical means. A chemical dehumidifier utilizes an adsorbent, such as silica gel, to remove unwanted moisture from the air. Mechanical dehumidification requires cooling coils utilizing chilled water, brine, or a refrigerant. The water vapor in the air condenses when it passes over the cooling coils that are cooled below the air dew point. The processed air is then supplied into the conditioned space. Normally, the supply air is cooled to the required specific humidity first and reheated to the required temperature subsequently if the accurate control of both space temperature and humidity is required.

The performance of a conventional split-type residential air-conditioner is dependent on adequate airflow across the evaporator coil to achieve a balance between the sensible heat transfer and the moisture removal (Parker et al., 1997). If the coil airflow is too high, air moisture removal is compromised and fan power input is increased. On the other hand, the sensible cooling capacity is reduced with degradation of the system energy efficiency ratio (EER) if the airflow is too low.

The temperature and humidity control in a direct cooling refrigeration plant has been studied (Krakow et al., 1995b). Their study showed that the sensible and latent components of the plant cooling capacity always increased with an increase in the compressor volumetric displacement rate. The latent cooling capacity component always decreased with an increasing evaporator airflow rate. The strategy of controlling the temperature by varying compressor speed and the humidity by varying fan speed was shown to be successful in their experiments. The other control strategy of controlling the temperature and the humidity by varying fan speed and compressor speed respectively failed. The reason for this is that the changes in sensible and latent cooling capacity components when the compressor volumetric displacement rate changes from its minimum to its maximum are greater than the corresponding changes when the evaporator airflow rate changes from its minimum to maximum. Since the sensible cooling load components are generally greater than the latent cooling load components, and changes in sensible cooling load components are generally greater than changes in latent cooling load components, it is more logical to control temperature by controlling compressor volumetric displacement and to control humidity by controlling the evaporator airflow rate.

In chilled water air-conditioning systems, the surface temperature of cooling coils is generally below the air dew point. In such a situation, the moisture content of the supply air falls after passing through the AHU due to condensation. Previous field studies have demonstrated that lowering the airflow rate across the cooling coil and lowering the evaporator coil temperature resulted in the air at the outlet having a lower moisture content (Khattar and Henderson, 1999; Shirey, 1993). The dehumidification improvement resulted from a lower airflow rate over the cooling coils, which decreased the coil bypass factor and allowed the outlet air temperature to more closely approach the coil temperature. Therefore, the latent cooling capacity of the air-conditioning systems can be modified by changing the supply airflow rate. It was observed that the airflow reduction decreased the room RH and significantly improved the indoor comfort conditions (Liu et al., 1999).

2.2 Control of Air-Conditioning Systems

Control theory deals with the analysis and synthesis of dynamic systems in which one or more variables are to be kept within prescribed limits. The problem of control is to design a controller, which generates the desired control action. This action is then applied to the system under control to drive it such that the response is satisfactory.

Since the early prototype of a PID controller emerged in the 1930s, it has been by far the most successful and widely used controller in industrial applications. Even now, when applications of digital control systems are widespread, the PID control remains important in numerous applications (Kasahara et al., 1999). This is because PID controllers are simple and proven to be reliable for field operatoration in the process industries. The air-conditioning system has complex dynamics with nonlinearity, distributed parameters, multi variables and is subject to external disturbances, such as

the weather variation and changing heat loads. It is thus difficult to obtain an accurate dynamic model of the system. The tuning of the PID parameters is then not an easy procedure because this is based on the system model.

Some researchers use approximate linear models to describe the air-conditioning system. Most HVAC systems are approximated by a first-order lag plus deadtime for simplicity. Because it is modeled based on some assumptions and around some operating point, the model is only applicable to the neighborhood of that point. About this operating point, it is possible to achieve satisfactory performance if the PID gains are properly tuned. This itself is a tedious and difficult process even for experienced field operators.

Even if a PID controller is properly tuned and give satisfactory performance about some designed operating condition, system performance degrades significantly and instability, in the form of hunting, can occur if the operating condition deviates much from the designed operating point. This behavior is attributed to the high non-linearity of the air-conditioning systems (Matsuba et al., 1998).

A HVAC system is a multi-input multi-output (MIMO) process with strong couplings between the variables. The control system normally requires multi loops, with parameters in each loop based on a SISO model. Kasahara et al. (1999) designed a robust PID controller design for HVAC systems. In his work, the components of the system were assumed as SISO systems and interactions among components were neglected. A multivariable feedback controller was proposed (He et al., 1998). His proposed controller achieved better performance compared to a SISO controller. But the model is of 11^{th} order and it should be linearized about a certain operating point.

Carlos and Miguel (2001) studied the control of temperature and relative humidity in a thermal space conditioned by a VAV system. When separate controllers were used for each variable and the coupling dynamics between these variables were not taken into account, it was impossible to set one without affecting the other. Carlos and Miguel used a decoupling technique to achieved accurate control. It was shown that the decoupled control of temperature and relative humidity was achieved using multivariable cascade control with two loops. The inner-loop was the non-interacting control law used for decoupling, and the outer-loop was a PD controller used for stabilization and control. However, the complexity is apparent in his design that requires knowledge of some system parameters that are not easy to determine. The method is model-specific and cannot be easily applied to other systems.

Adaptive control techniques have been proposed to replace the classical methods. The ability to adapt to variations in plant dynamics and environment automatically has made the adaptive controllers increasingly important for various applications. Before they can be implemented, however, mathematical modeling of the plants has to be done, which is sometimes difficult and laborious. In addition, inaccuracy in the modeling of the plant leads to degraded performance of the controllers (Khalid et al., 1995).

Recent research has focused on developing model-free control systems. Some intelligent control techniques were introduced, including knowledge-based systems, fuzzy logic and neural networks. The related work will be reviewed in the following section.

2.3 Fuzzy Logic Control

Based on Zadeh's theory of fuzzy sets, the concept of fuzzy logic has been successfully applied to the control of industrial processes particularly those that are ill-defined but which can be successfully controlled by human operators.

The basic idea of this approach is to incorporate the experience of human operators in the design of the controllers. The value of the inputs and outputs need not be numerical and may be expressed in natural language. Most commonly, a fuzzy logic model includes a mapping of input values to output values using simple *IF-THEN* statements, such as *"IF room temperature is high, THEN supply more cool air to the room"*. These types of mappings permit the incorporation of expert knowledge with the fuzzy logic model.

2.3.1 Fuzzy If-Then Rule

Assuming there are two inputs, x and y, to the system and the output is z. An example of a fuzzy if-then rule is:

If x is A_i and y is B_i, then z is C_i.

where x, y and z are linguistic variables, A_i, B_i and C_i are fuzzy sets characterized by membership functions.

Another form of fuzzy if-then rule, T-S type proposed by Takagi and Sugeno (1985), has fuzzy sets involved only in the antecedent.

If x is A_i and y is B_i, then $z = c_{0i} + c_{1i}x + c_{2i}y$

where the consequent of the rule is a linear function of the input variables.

A simpler form is extensively used, which is actually a zero order T-S fuzzy rule.

If x is A_i and y is B_i, then $z = z_i$

where z_i is a crisply defined number.

Through the use of linguistic labels and membership functions, a fuzzy if-then rule can easily capture the essence of human's experience. Fuzzy if-then rules form the core of the fuzzy inference system to be introduced below.

2.3.2 Fuzzy Reasoning

Fuzzy reasoning is an inference procedure used to derive conclusions from a set of fuzzy if-then rules and one or more conditions. The steps of fuzzy reasoning performed by fuzzy inference systems are (Shaw, 1998):

- Compare the input variables with the membership functions in the antecedent to obtain the membership values of each linguistic label (fuzzification).
- Combine the membership values on the antecedent to get firing strength (weight) of each rule.
- Generate the qualified consequent of each rule depending on the firing strength.
- Aggregate the qualified consequent to produce a crisp output (defuzzification).

2.3.3 Fuzzy Inference System

Basically, a fuzzy inference system is composed of four functional blocks as shown in Fig. 2-1 (Jang, 1993):

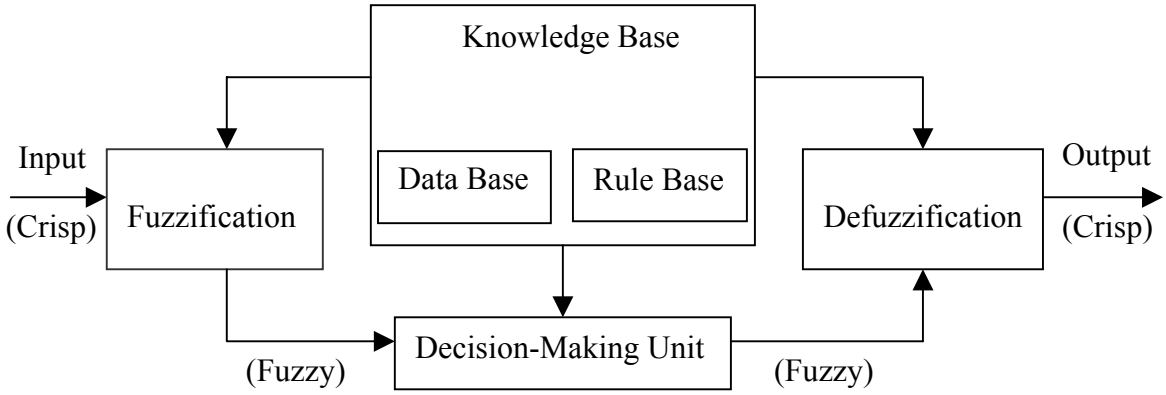

Figure 2-1 Basic fuzzy inference system

- A fuzzification interface which transforms the crisp inputs into degrees of match with linguistic values.
- A knowledge base which contains a number of fuzzy if-then rules and defines the membership functions of fuzzy sets used in the fuzzy rules.
- A decision-making unit, sometimes referred to as an inference engine, which performs the interface operations on the rules.
- A defuzzification interface which transforms the fuzzy results into crisp outputs.

Depending on the types of fuzzy reasoning and fuzzy if-then rules employed, fuzzy inference systems can be classified into different types:

- Mamdani fuzzy inference system:

  The overall fuzzy output is derived by applying "max" operation to the qualified fuzzy outputs (each of which is equal to the minimum of firing strength and the output membership function of each rule). The centroid of area, bisector of area and mean of maximum are normally used to obtain the final crisp outputs from the fuzzy outputs.

- Takagi-Sugeno fuzzy inference system:

  This system is applicable for Takagi-Sugeno type rules. The final outputs are the weighted average of each rule's outputs. When the consequent of rules are crisp value, the overall outputs are the weighted average of each rule's crisp outputs.

The following features have effect on the performance of fuzzy logic controllers (FLCs) (Pedrycz, 1989).

- Scaling factors for input and output variables.
- Membership functions of fuzzy sets.
- Setting of fuzzy rules.

2.3.4 Applications to Air-Conditioning Systems

Huang & Nelson (1991) combined a PID controller with a FLC and applied it to a general second-order plant model. The fuzzy sets were developed for control error, integral error and derivative error (essentially the terms of a PID controller) and an output set for the control signal. The computer simulations showed that the combined controller virtually eliminated the damped oscillations common with tuned conventional PID control as well as achieved faster response.

A FLC was applied to the control of an air handling plant in VAV systems (So et al. 1994 and 1997). Using triangular membership functions for error and error rate, FLC outputs were generated for the air handling plant fresh air damper, fan, cooling coil, humidifier and reheat coil. The performance was compared with tuned and detuned PID control using computer simulations. It was shown that the FLC compared well with the tuned PID control but was more robust and the FLC was superior (in terms of

response time and offset) to the detuned PID control. FLC has also been successfully used in the control of temperature and humidity (Becker et al., 1994; Arima et al., 1995). However, all these results were obtained from pure computer simulations. Because practical systems may deviate significantly from the mathematical models used in computer simulations, it is necessary to implement the controller in actual experiments to ascertain the performance of FLCs.

2.4 Artificial Neural Networks

One of the most important capabilities of an artificial neural network (ANN) is that it can be trained to do a mapping between input and output variables by adjusting a set of weights and thresholds of a connectionist model based on training examples. It attempts to achieve good performance through massive interconnections of simple computational elements or neural units. An artificial neural network model is characterized by its architecture, its processing algorithm and its training algorithm. The network architecture specifies the arrangement of neural connections while the type of units is characterized by the activation function used. For a given architecture, the neural network is used in two different modes: the processing mode and the training mode. In the processing mode, the processing algorithm specifies how the neural units compute the outputs for any set of inputs and for a given set of weights. The training algorithm specifies how the neural network adapts its weights for all training patterns (Haykin, 1999).

With respect to the architecture, four main types of neural networks can be distinguished:

- Layered feed-forward neural networks, where a layer of neurons receive inputs only from the neurons from the previous layer, such as multi-layer perceptrons.

- Recurrent neural networks, where the inputs to neurons are the net's previous outputs as well as inputs from external sources.
- Laterally connected neural networks, which consist of feedback input units and a lateral layer consisting of such neurons that are laterally connected to their neighbors.
- Hybrid networks, which combine two or more of the above features.

The training algorithms for neural networks can be classified into supervised learning and unsupervised learning. In supervised learning, the networks are presented with a set of example input-output pairs and trained to implement a mapping that matches the examples as closely as possible. In contrast, for unsupervised learning, the networks are presented with only the input samples, and learned to group these samples into classes that have similar feature.

2.4.1 Multi-Layer Perceptron

The multi-layer perceptron (MLP) is the most used and studied artificial neural network. According to the Kolmogorov theorem (Kolmogorov, 1957), a three-layer perceptron can be trained to approximate any non-linear function. Thus, the MLP can be a suitable tool for obtaining good approximate solutions in complicated mapping problems.

A MLP is formed from interconnections of many basic neurons and are typically of the structure shown in Fig. 2-2. As shown in Fig. 2-2, in addition to the necessary input layer and output layer, there is also a hidden layer. This structure is referred to as a three-layer network in this work because it has three layers of nodes. However, it has only two layers of processing elements, the hidden layer and the output layer.

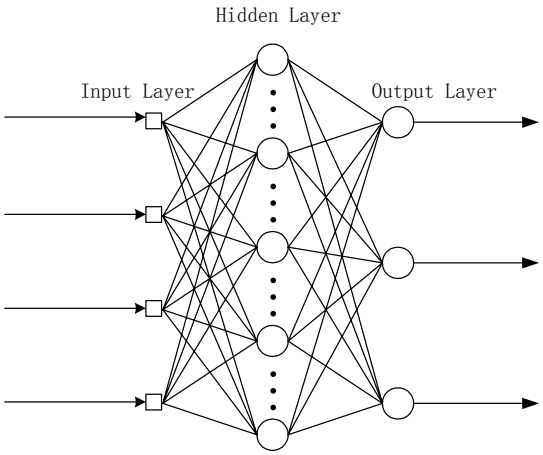

Figure 2-2 Simple architecture of a multi-layer perceptron

In these layers, each neuron in a layer is connected to neurons in the previous and in the next layer, but it is not connected to any neuron in the same layer. These connections between neurons have their adjustable weights, which are adjusted during the training process. The inputs to each processing neuron are multiplied by their corresponding weight and the weighted sum is then acted upon by an activation function before the output.

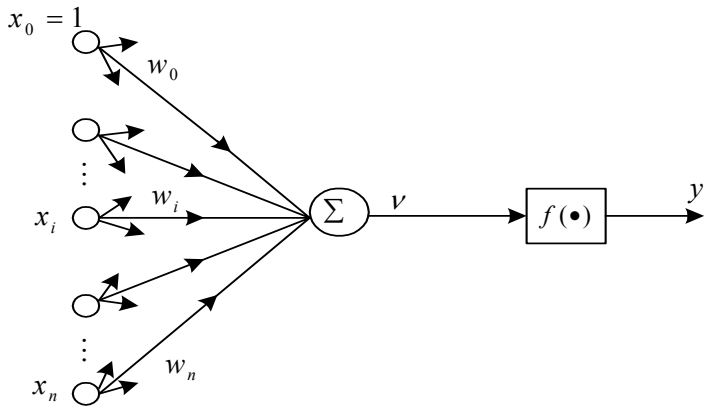

Figure 2-3 Structure of a neuron

Fig. 2-3 shows the structure of a single neuron. The function of the neuron can be described by

$$v = \sum w_i x_i \tag{2-1}$$

$$y = f(v) \tag{2-2}$$

where y is the output of the neuron,

x_i, $i = 0,\ldots,n$ are the n inputs to the neuron,

w_i, $i = 0,\ldots,n$ are the weights connecting the input x_i to the neuron, and

$f(\bullet)$ is the activation function which operates on the weighted sum of input, v.

Typically, in addition to the inputs, a bias input is also added. If x_0 is used as the bias input, it is normally set to a constant value of 1 and the bias is adjusted during training through adjustment of the bias weight w_0.

The following activation functions are commonly used:

- Threshold function:

$$f(v) = \begin{cases} 1, & v \geq 0 \\ 0, & v < 0 \end{cases} \tag{2-3}$$

- Sigmoid function (shown in Fig. 2-4):

(unipolar) $$f(v) = \frac{1}{1+e^{-v}} \tag{2-4}$$

or, (bipolar) $$f(v) = \frac{1-e^{-v}}{1+e^{-v}} \tag{2-5}$$

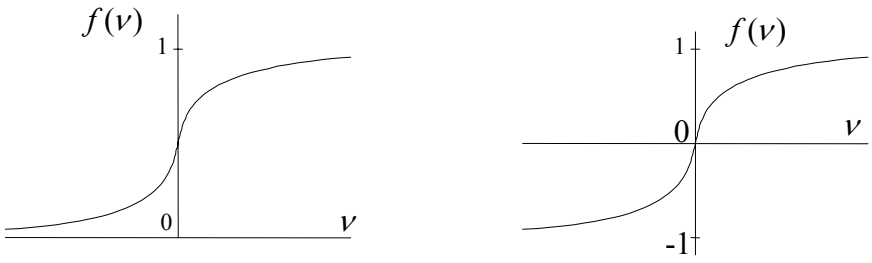

(a) Unipolar (b) Bipolar

Figure 2-4 Sigmoid functions

2.4.2 Back-Propagation Learning Algorithm

The MLP is a supervised-training neural network, that is, its training process requires training pairs consisting of the input vectors and the corresponding desired output vectors. Upon each presentation of a training pair, the connecting weights are adjusted to reduce the difference between the target or desired outputs and the actual outputs of the network. The training set, comprising many training pairs, is presented to the neural network repeatedly until the error decrease below the desired level. Study of different learning algorithms is always a very active area of the research in artificial neural networks. To date, many algorithms have been developed, among which the back-propagation (BP) algorithm is the most widely used.

Before the BP algorithm is derived, the following notations are introduced:

$y_j^l(p)$	output of the jth node in layer l for the pth training example
$net_j^l(p)$	net input to the jth node in layer l for the pth training example
$w_{ji}^l(p)$	weight connecting the ith node in layer $l-1$ to the jth node in layer l for the pth training example
$d_j(p)$	desired response of the jth output node for the pth training example
$\delta_j^l(p)$	local gradient for jth node in layer l for the pth training example
N_l	number of nodes in layer l
L	number of layers
P	number of training examples

The nodes in the first layer only transmit the inputs to the second layer. Referring to Fig. 2-3, the output of a node in layer l, for $l \geq 2$, is given by

$$y_j^l(p) = f(net_j^l(p)) \tag{2-6}$$

where

$$net_j^l(p) = \sum_{i=0}^{N_{l-1}} w_{ji}^l(p) y_i^{l-1}(p) \tag{2-7}$$

For the special cases, we have

$y_i^1(p)$ is the ith component of the input vector to the network

$y_0^{l-1}(p) = 1$, and $w_{j0}^l(p)$ is the bias weight

$f(\bullet)$ is the activation function.

BP uses a gradient search technique to find the network weights that minimize an objective function. The objective function to be minimized is usually the average squared error function:

$$J_{av} = \frac{1}{P}\sum_{p=1}^{P} J(p) \tag{2-8}$$

where $J(p)$ is the total squared error at the output layer for the pth example:

$$J(p) = \frac{1}{2}\sum_{j=1}^{N_L} (d_j(p) - y_j^L(p))^2 \tag{2-9}$$

where N_L is the number of nodes in the output layer.

The weights of the network are determined iteratively according to:

$$w_{ji}^l(p+1) = w_{ji}^l(p) + \Delta w_{ji}^l(p) \tag{2-10}$$

$$\Delta w_{ji}^{l}(p) = -\eta \frac{\partial J(p)}{\partial w_{ji}^{l}(p)} \tag{2-11}$$

where η is a positive constant called the learning rate. To implement this algorithm, an expression for the partial derivative of $J(p)$ with respect to each weight in the network is developed. For an arbitrary weight in layer l, this can be computed using the chain rule:

$$\frac{\partial J(p)}{\partial w_{ji}^{l}(p)} = \frac{\partial J(p)}{\partial y_{j}^{l}(p)} \frac{\partial y_{j}^{l}(p)}{\partial w_{ji}^{l}(p)} \tag{2-12}$$

$$\frac{\partial y_{j}^{l}(p)}{\partial w_{ji}^{l}(p)} = \frac{\partial}{\partial w_{ji}^{l}(p)} [f(net_{j}^{l}(p)]$$

$$= f'(net_{j}^{l}(p)) \frac{\partial}{\partial w_{ji}^{l}(p)} \left[f(\sum_{i=0}^{N_{l-1}} w_{ji}^{l}(p) y_{i}^{l-1}(p)) \right]$$

$$= f'(net_{j}^{l}(p)) y_{i}^{l-1}(p) \tag{2-13}$$

The local gradient $\delta_{j}^{l}(p)$ is defined by

$$\delta_{j}^{l}(p) = -\frac{\partial J(p)}{\partial net_{j}^{l}(p)} \tag{2-14}$$

If layer l is the output layer, $l = L$,

$$\delta_{j}^{L}(p) = (d_{j}(p) - y_{j}^{L}(p)) f'(net_{j}^{L}(p)) \tag{2-15}$$

If layer l is a hidden layer,

$$\delta_{j}^{l}(p) = f'(net_{j}^{l}(p)) \sum_{k} \delta_{k}^{l+1}(p) w_{kj}^{l+1}(p) \tag{2-16}$$

where the kth neuron in the $l+1$ layer is connected to the jth neuron. Finally, the correction $\Delta w_{ji}^{l}(p)$ is defined by:

$$\Delta w_{ji}^{l}(p) = \eta \delta_{j}^{l}(p) y_{i}^{l-1}(p) \qquad (2\text{-}17)$$

The above equations comprise the back-propagation learning algorithm. At the beginning of the training process, all the connecting weights are usually initialized to some small random values. The learning rate can be fixed or adaptively chosen in a number of ways. The process of computing the gradient and adjusting the weights is repeated until the output error decrease to some specified level. The multi-layer perceptron can be used as a universal approximator, a classifier or a regression machine.

2.4.3 Applications to Air-conditioning Systems

Curtiss et al. (1994) used a back-propagated feedforward ANN with two hidden layer each of 10 neurons for energy management in a central plant, concluding that the ANN can be successfully used to model energy use as well as to carry out energy management tasks, such as set point resetting. Huang and Nelson (1994) trained an ANN to determine the delay time of a HVAC plant (an accurate knowledge of plant dead time can be used to improve control performance). They also used a four-layer architecture, with two hidden layers, which is trained using the delta rule back-propagation. Besides successfully predicting the delay time, the ANN was found to be able to tolerate different levels of input measurement noise.

HVAC control applications of ANNs have received some attention recently. Ahmed et al. (1996) applied a simplified ANN architecture, the general regression neural network (GRNN), to identify and control a plant involving a heating coil and a valve. In this application, the GRNN was used to identify the static plant characteristics for use in feedforward compensation. Ding and Wong (1990) used an ANN for the control of valves in a complex heating and cooling network based on simulated operating data.

Several researchers have trained ANNs to act as compensators to improve conventional feedback controls. Curtiss et al. (1993) developed an ANN-based predictive controller as an alternative to the conventional PID control. Curtiss et al. (1996) developed a 'look-ahead' network adaptive ANN in which plant error was back-propagated through the ANN in a Hopfield-like fashion and the network was used to predict future plant behavior as a basis for control action. The resulting controller was found to be at least as good as a well-tuned PID control but was critically dependent on the choice of the network learning rate used.

So et al. (1995) developed a combined identifier/controller for a MISO application in which control of an air handling plant was considered using an ANN. They compared the ANN with a well-tuned PID and a fuzzy logic controller, concluding that the response rate of the ANN-based method was inferior to the fuzzy logic controller and steady state accuracy was slightly inferior to a well-tuned PID. However, the design of the ANN controller was straightforward and the controller did not require any tuning or any expert knowledge.

2.5 Integration of Fuzzy Logic and Neural Networks

Fuzzy logic and neural networks have been briefly overviewed in the previous sections. Table 2-1 lists the characteristics of fuzzy logic and neural networks. It can be seen that fuzzy logic and neural networks have several characteristics in common. For example, both are model-free function estimators that can be adjusted or trained for improved performance. However, each has its own advantages. The advantages of fuzzy logic over neural network are its tolerance for imprecision and explicit knowledge representation. On the other hand, neural networks offer other advantages such as the ability to learn and to generalize from these. In this regard, it is believed

that the integration of fuzzy logic and neural networks can leverage the advantages of the two individual techniques.

Table 2-1 Characteristics of fuzzy logic and neural networks (Medsker, 1995)

Properties of intelligent systems	Fuzzy logic	Neural Networks
Function estimators	√	√
Trainable, dynamic	√	√
Improvement with use	√	√
Parallel implementation	√	√
Numerical	√	√
Tolerance for imprecision	√	
Explicit knowledge representation	√	
Adaptive		√
Optimising		√
Interpolative		√
Tolerance for noise		√

Research in the use of fuzzy logic with neural networks has been progressing at a rapid pace during the last few years. The integration of fuzzy logic and neural networks can be viewed from different perspectives. In terms of applications, numerous studies have been done on the improvement of control systems, conventional or fuzzy, by use of the neural technology. Other applications modify neural networks, supervised or unsupervised, with fuzzy techniques to improve their performance. The main approaches to integration of fuzzy logic and neural networks can be summarized as follows: fuzzy connectionst expert system, neural networks for designing and tuning fuzzy systems, FAM (fuzzy associative memory), FCM (fuzzy cognitive map) and FNN (fuzzy neural networks).

CHAPTER 3
AIR-CONDITIONING SYSTEM MODELING

In hot and humid countries like Singapore, air-conditioning plants are usually employed for cooling and dehumidification purposes. A commercial chilled-water all-air system was studied in this project. Experiments were conducted on this system to investigate the proposed control method. The control strategy must be analyzed theoretically prior to implementation. This chapter presents the principles of the air-conditioning system and the modeling of its main components.

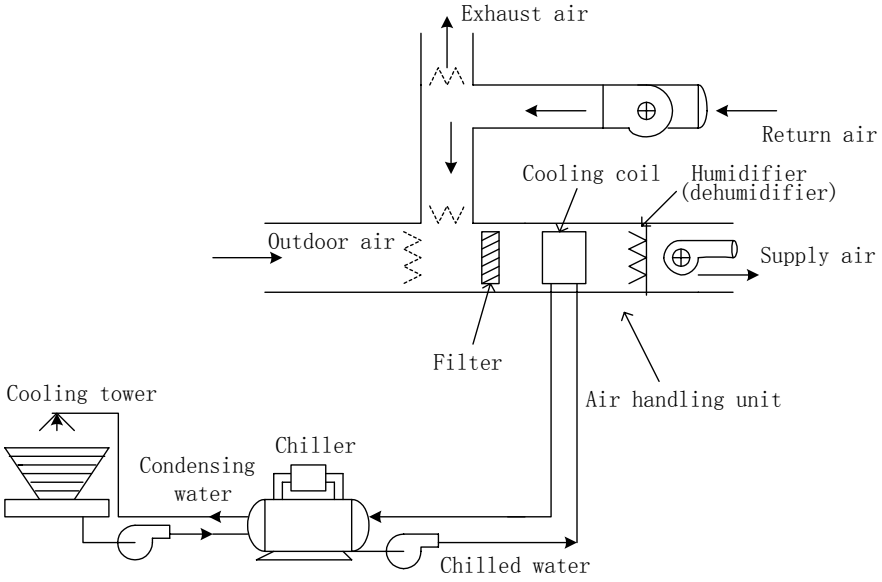

Figure3-1 Schematic diagram of a chilled water air-conditioning system

Fig. 3-1 is a schematic diagram showing the major elements of a commercial air-conditioning system. The chiller, which produces the chilled water, is the source of system cooling capacity. The chilled water is supplied to the cooling coils in the air-handling unit (AHU) where the water extracts heat from the passing air. The processed

air is then supplied to the conditioned space. In this way, the space is maintained at the desired condition. Because the heat transfer between the chilled water and air occurs in the AHU, its performance directly decides the system cooling capacity.

3.1 Modeling of the Air-Handling Unit

The cooling coils play the main role in the AHU because the humidifier (dehumidifier) is not used in this work. The chilled water flows inside the cooling coils, and the air passes over the coils. When the moist air passes over a surface so that the air stream is cooled below its dew point, some of the water vapor will condense. In this case, both sensible cooling and dehumidification are achieved. The process can be plotted on the psychrometric chart (Jones, 1994).

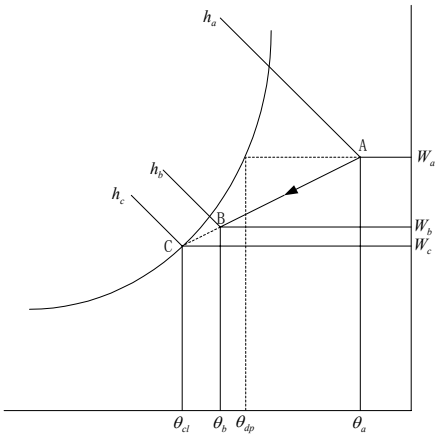

Figure 3-2 Cooling and dehumidifying process

Fig. 3-2 shows the process in which the moist air is cooled and dehumidified. The moist air enters the cooling coils at state A, corresponding to a dry-bulb temperature θ_a and humidity ratio W_a. The apparatus dew point θ_{cl}, which is also sometimes termed the mean coil surface temperature, is below the moist air dew point θ_{dp}. With the water vapor condensing, the air leaves the cooling coils at state B, corresponding to

a dry-bulb temperature θ_b and humidity ratio W_b. The air temperature and moisture content both decrease. It has been demonstrated that as the air velocity is reduced, the coil condition curve drawn on the psychrometric chart becomes steeper, indicating an increase in the dehumidification per unit of sensible cooling (Chew, 1994).

The heat transfer through the tube wall can be illustrated in a simple form by the schematic diagram in Fig. 3-3. The actual process may vary considerably depending on the type of surface, surface temperature, and flow conditions. Heat is transferred from the air to the chilled water through the tube wall. The heat flow rate is decided by the heat transfer coefficients of both sides. The ratio of the heat transfer coefficient of the chilled water side to that of the air side determines the surface temperature of the coil. When the ratio is large, the coil surface temperature θ_{cl} is biased towards the chilled water temperature. There is then a higher rate of condensation of moisture from the air (Chew, 1994).

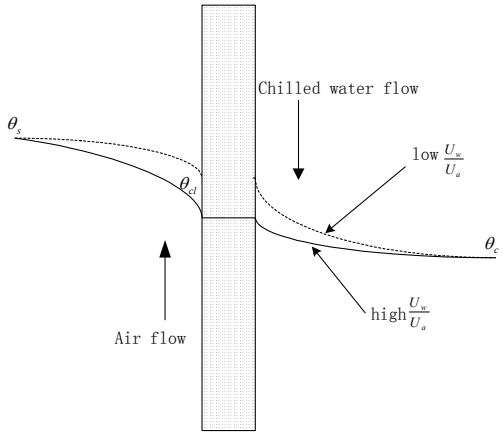

Figure 3-3 Simple illustration of heat transfer in cooling coils

If the heat transfer coefficient U_a of the air side is large due to a high airflow rate, or if the heat transfer coefficient U_w of the chilled water side is small due to a low chilled water flow rate, the coil surface temperature θ_{cl} will be biased towards the air

temperature. This may then be too high relative to the air dew point for any condensation of the moisture in the air to occur.

In what follows, we will analyze the cooling coils as a whole. Fig. 3-4 shows the schematic diagram of a cooling coil.

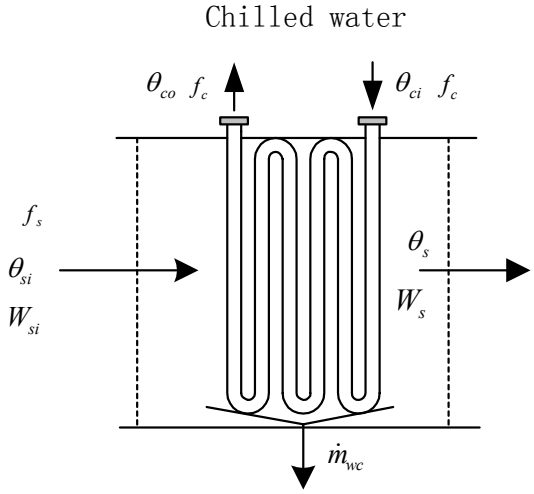

Figure 3-4 Schematic diagram of a cooling coil

In order to model the cooling coil, it is assumed that the air, at a flow rate of f_s, enters the cooling coil at a temperature θ_{si} and humidity ratio W_{si}. It is also assumed that the air within the cooling coil unit has a uniform density, of a uniform temperature θ_s and a uniform humidity ratio W_s. The chilled water at temperature θ_{ci} is supplied to the cooling coil and returns at a temperature of θ_{co}. By identifying the energy flows to and from the air-handling unit, the energy balance can be expressed as (Kasahara et al., 2000):

$$C_a \frac{d\theta_s}{dt} = f_c \rho_w c_w (\theta_{ci} - \theta_{co}) + \alpha_a (\theta_o - \theta_s) + f_s \rho_a c_a (\theta_{si} - \theta_s) \qquad (3\text{-}1)$$

where

C_a = air handling unit air thermal capacity

f_c = chilled water flow rate

ρ_w = density of the chilled water

c_w = chilled water specific heat

c_a = air specific heat

ρ_a = air density

α_a = unit area-integrated heat transfer coefficient

In Eq.3-1, the rate of increase in energy stored in the unit is equated to the energy supplied by the chilled water and the energy added to the unit via the return air from the room and the surrounding outer surface of the unit. The mass balance equation on the water vapor is:

$$V_a \frac{dW_s}{dt} = f_s (W_{si} - W_s) \qquad (3\text{-}2)$$

From Eq.3-1, a lower supply air temperature can be achieved by increasing the chilled water flow rate or decreasing the airflow rate. Eq.3-2 implies that, by changing the supply airflow rate, the water vapor can be stored in the air-handling unit. Previous field studies have showed that lowering airflow across the cooling coil can enhance the moisture removal rates. Luxton and Shaw (1991) assessed the impact of variable air velocity and chilled water flow on the coil performance using program simulations. It was found that changes in the chilled water flow and air velocity led to great changes in the ratio of the latent heat transfer to the sensible heat transfer.

3.2 Modeling of the Conditioned Room

A simple energy balance for the room air can be written (Underwood, 1999):

$$C_r \frac{d\theta_r}{dt} = q_{plant} - \sum (AU_i)(\theta_r - \bar{\theta}_f) - \frac{n_v V_r}{3}(\theta_r - \theta_o) + q_{gain} \qquad (3\text{-}3)$$

where

C_r = room air thermal capacity (product of volume, density and specific heat) (JK^{-1})

θ_r = room air temperature (℃)

q_{plant} = energy input from plant (W)

$\bar{\theta}_f$ = the surface temperature of the room fabric (℃)

$\sum (AU_i)$ = area-integrated fabric surface heat transfer coefficient (WK^{-1})

$n_v V_r / 3$ = ventilation coefficient (WK^{-1}) in which n_v, V_r are ventilation air change (h^{-1}) and room volume (m^3) respectively

θ_o = external temperature (℃)

q_{gain} = room sensible heat gain (W)

Substituting for $C_r = V_r \rho_a c_a$ and expressing each term as a deviation rather than an absolute value, the constant terms in the equation disappear and Eq.3-3 is then expressed by:

$$V_r \rho_a c_a \frac{d(\delta\theta_r)}{dt} = \delta q_{plant} - (\sum (AU_i) + \frac{n_v V_r}{3})\delta\theta_r \qquad (3\text{-}4)$$

where notation δ implies deviations in the variables from some known steady state values.

Taking Laplace transform on both sides, the room air temperature to the plant heat input transfer function is:

$$\frac{\theta_r(s)}{q_{plant}(s)} = \frac{K_r}{\tau_r s + 1} \tag{3-5}$$

where

$$\tau_r = \frac{V_r \rho_a c_a}{\sum (AU_i) + n_v V_r / 3} \tag{3-6}$$

$$K_r = \frac{1}{\sum (AU_i) + n_v V_r / 3} \tag{3-7}$$

Eq.3-3 is a linear differential equation, which contains no function of variables such as exponentiation or product of two or more variables. However, the plant cooling capacity is determined by the supply air temperature and flow rate in VAV systems.

$$q_{plant} = m_a c_a (\theta_s - \theta_r) \tag{3-8}$$

The product of supply air mass flow rate, supply air temperature and room temperature, all of which may vary, presents non-linearity. About the initial steady condition,

$$\delta q_{plant} \cong \delta m_a c_a (\theta_{si} - \theta_{ri}) + \delta \theta_s m_{ai} c_a - \delta \theta_r m_{ai} c_a \tag{3-9}$$

where subscript i refers to the initial steady state.

Substituting Eq.3-9 in Eq.3-4, the following room model is finally obtained:

$$\theta_r(s) = \frac{K_{m_a}}{\tau_r s + 1} m_a(s) + \frac{K_{\theta_s}}{\tau_r s + 1} \theta_s(s) \tag{3-10}$$

where

$$\tau_r = \frac{C_r}{m_{ai}c_a + \sum(AU_i) + n_v V_r/3} \tag{3-11}$$

$$K_{m_a} = \frac{c_a(\theta_{si} - \theta_{ri})}{m_{ai}c_a + \sum(AU_i) + n_v V_r/3} \tag{3-12}$$

$$K_{\theta_s} = \frac{m_{ai}c_a}{m_{ai}c_a + \sum(AU_i) + n_v V_r/3} \tag{3-13}$$

Eq.3-3 through Eq.3-13 describe the dynamics of the sensible heat transfer process. The air-conditioning plant also provides dehumidification. The moisture transfer in a space is more complicated due to long-term moisture absorption/desorption in the fabric of the space. If the fabric effect is neglected, the moisture balance for the room can be expressed as:

$$V_r \rho_a \frac{dW_r}{dt} = m_a(W_s - W_r) - \frac{n_v V_r \rho_a}{3600}(W_r - W_o) + m_{gain} \tag{3-14}$$

where

W_r = room humidity ratio

W_s = supply air humidity ratio

W_o = external humidity ratio

m_{gain} = room moisture gain

Similar to Eq.3-9,

$$m_a(W_s - W_r) \cong m_a(W_{si} - W_{ri}) + m_{ai}W_s - m_{ai}W_r \tag{3-15}$$

Substituting it in Eq.3-14, the following equation is finally obtained,

$$W_r(s) = \frac{K_{m_a}}{(\tau_{W_r} s + 1)} m_a(s) + \frac{K_{W_s}}{(\tau_{W_r} s + 1)} W_s(s) \quad (3\text{-}16)$$

where

$$\tau_{W_r} = \frac{V_r \rho_a}{(m_{ai} + n_v V_r \rho_a / 3600)} \quad (3\text{-}17)$$

$$K_{m_a} = \frac{(W_{si} - W_{ri})}{(m_{ai} + n_v V_r \rho_a / 3600)} \quad (3\text{-}18)$$

$$K_{W_s} = \frac{m_{ai}}{(m_{ai} + n_v V_r \rho_a / 3600)} \quad (3\text{-}19)$$

From Eq.3-10 and 3-16, it is clearly shown that the room temperature θ_r and humidity ratio W_r change with the supply air temperature θ_s, humidity ratio W_s and flow rate m_a. At the same time, from the equations for the cooling coils, we know that θ_s and W_s are functions of the airflow rate m_a and the chilled water flow rate m_w.

In VAV systems, a variable amount of air is supplied to space to meet the varying heat loads. It has been revealed that the reduction in the airflow rate greatly decreased the building relative humidity level (Liu et al., 1999). On the other hand, the room temperature is controlled by changing the chilled water flow rate in CAV systems. It shows that the chilled water flow rate also influences the system cooling capacity. These examples suggest that the strategy of controlling room temperature and relative humidity by varying chilled water flow and airflow rate is theoretically feasible.

3.3 Experimental Validation

Before examining the responses of the closed loop system, it is instructive to check the open loop responses of the system.

3.3.1 Experimental Air-Conditioning System

A simple diagram of the experimental system is depicted in Fig. 3-5. A fan and a motor equipped with a variable speed drive (VSD) are installed in the AHU to provide a variable airflow rate. The frequency of the input electrical power to VSD, from 0-37.5Hz, is modulated by a frequency converter, thereby allowing speed of the fan motor to be varied. The flow rate of the air is assumed to be linearly proportional to the fan speed. Variable airflow rates are passed through the cooling coils by varying the fan speed. Two three-way regulating valves are appended to the chilled water pipe. The valves are used in conjunction with an actuator to provide completely close to fully open operation. The actuator's 0-10 VDC signal corresponds to the valve's 0-100% opening. Varying the valve opening modifies the chilled water flow rate to the AHU, 100% opening corresponding to the maximum flow rate.

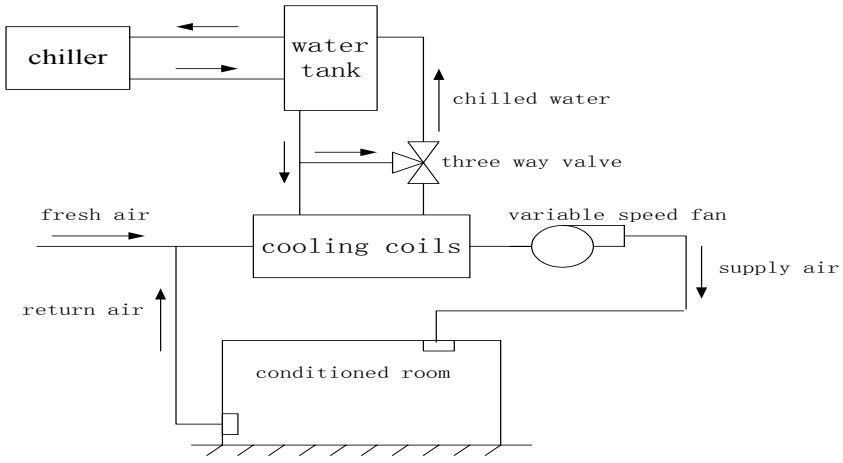

Figure 3-5 Simple diagram of the experimental air-conditioning system

An electrical resistance heater and a humidifier (The humidifier is simply a container of heated water) are used to simulate the sensible and latent heat load in the conditioned room respectively. The heat quantity emitted from the electrical heater can be varied by resetting the temperature of the thermostat. Two sensors are installed at the end of the supply air duct. These are capable of measuring the air temperature and relative humidity. The room temperature and RH are measured by two RTD sensors.

The start and stop operation of the chiller and dampers are performed by a Metasys building management system. A 200 MHz PC with an ISA bus Servo To Go interface card is used for the experiments. The supply air temperature and RH, and the room temperature and RH are sensed and recorded as well as the valve openings and fan speeds. The PC performs the data acquisition and controls the frequency converter and valve actuators. The detailed system information is depicted in Appendix A.

3.3.2 Supply Air Response

Some initial experiments were conducted to determine the responses of the supply air temperature and humidity to changes in supply airflow rate and chilled water flow rate. Fig. 3-6 shows the responses of the supply air temperature and RH when the VSD frequency was changed quickly from 20Hz to 35Hz, corresponding to a fan speed change from 1200 to 2100 rpm. The supply air temperature θ_s rose from 15.2℃ to 17.5℃ and the supply air RH ϕ_s increased from 90% to 97%. From the two responses, it can be concluded that the humidity ratio W_s of the supply air increased significantly after the fan speed change because its temperature and RH both increased.

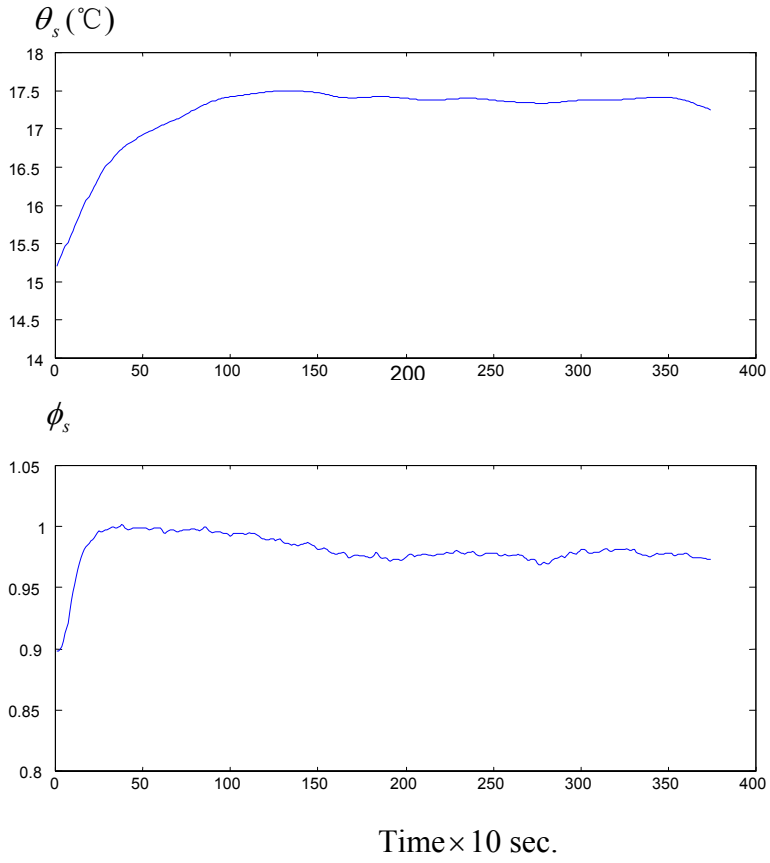

Figure 3-6 Supply air response to a step change in airflow rate

The chilled water flow rate was changed in the subsequent experiment. The supply air temperature and RH were recorded and are as shown in Fig. 3-7 when the chilled water valve opening was changed quickly from 50% to 100%. It can be clearly observed that a larger chilled water flow rate resulted in a lower supply air temperature, decreasing from 12.7℃ to10.5℃.

It can be seen in Fig. 3-7 that the supply air RH decreased first and increased approximately to the initial value when being steady again. Actually, the supply air RH (or humidity ratio) decreased very quickly as the chilled water flow rate was changed. Because the time constant of the RH sensor is about 2 minutes, it can be seen that the RH decreased to the lowest value at about t=120sec in this figure. After that, the air RH increased because of the decrease in the air temperature. Although the supply air

RH remained almost unchanged from its initial value to its value at the subsequent steady state (e.g. at t=1500sec), the supply air humidity ratio would have decreased significantly because of the lower supply air temperature.

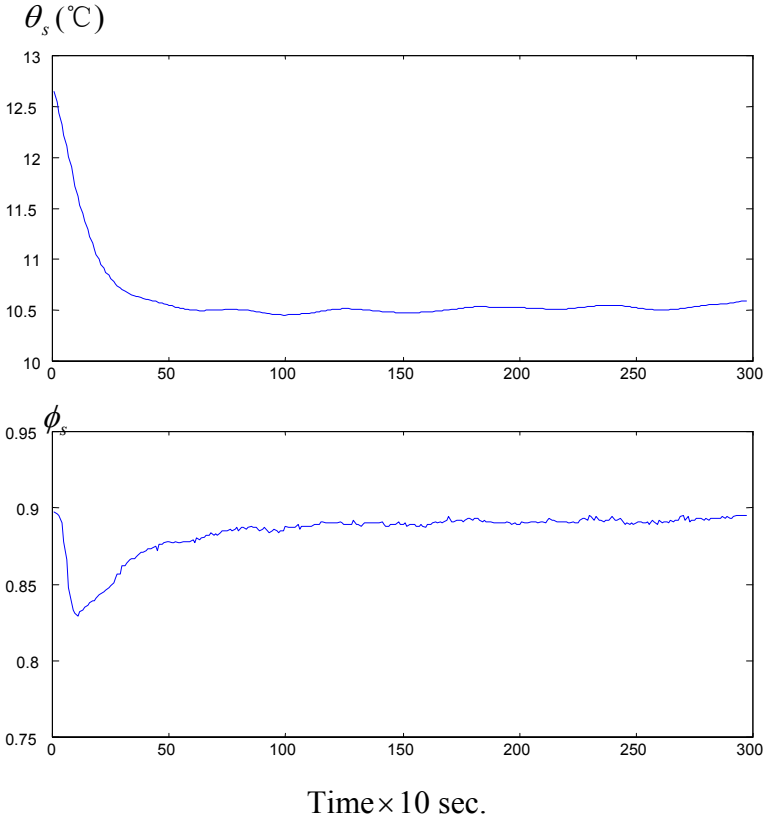

Figure 3-7 Supply air response to a step change in chilled water flow rate

3.3.3 Room Temperature and Relative Humidity Response

Step changes in the supply airflow rate and chilled water flow rate were made and the room temperature and RH were recorded in the following experiments. The room has already been in equilibrium at 19.6℃ and 61% before the change. The chilled water valves were closed from 100% to 50% opening while the fan speed was kept at 2100rpm. The responses of the room temperature and RH are shown in Fig. 3-8. It can be seen that the room temperature and RH increase to the new steady state values of 20 ℃ and 67%, respectively.

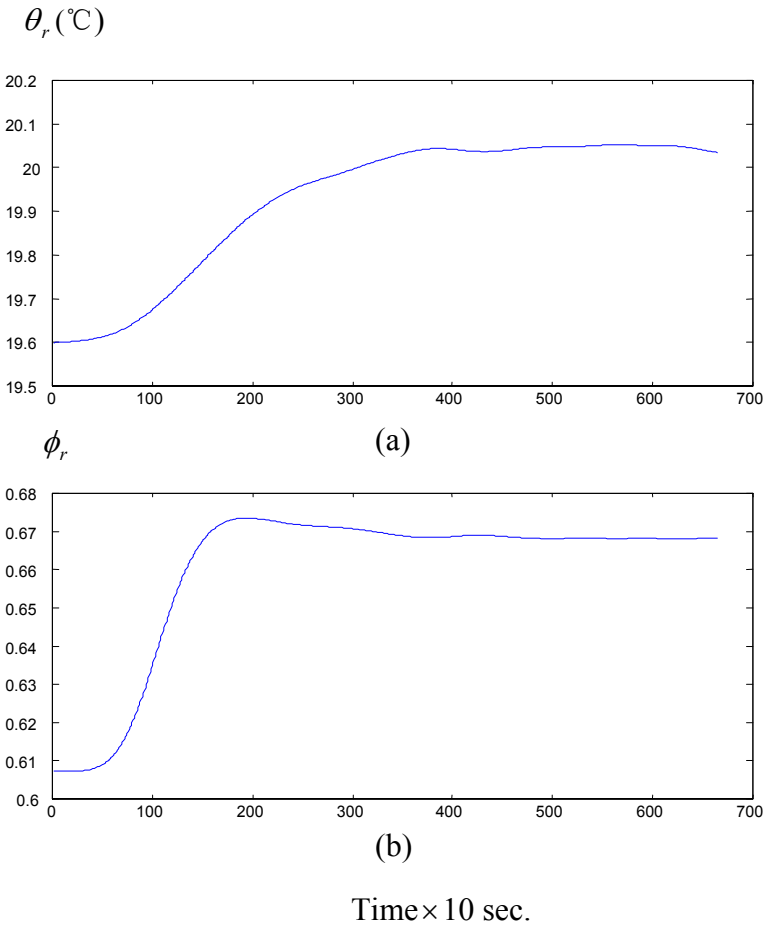

Figure 3-8 Room temperature and RH response to a step change in chilled water flow rate

Referring to Fig. 3-7, a reduction in valve opening, corresponding to a lower chilled water flow rate, results in a higher supply air temperature and higher moisture content. As a result, the room temperature and RH both increase because the supply airflow rate remains constant. It means that the lower chilled water flow rate reduces the cooling capacity of the system, both sensible and latent.

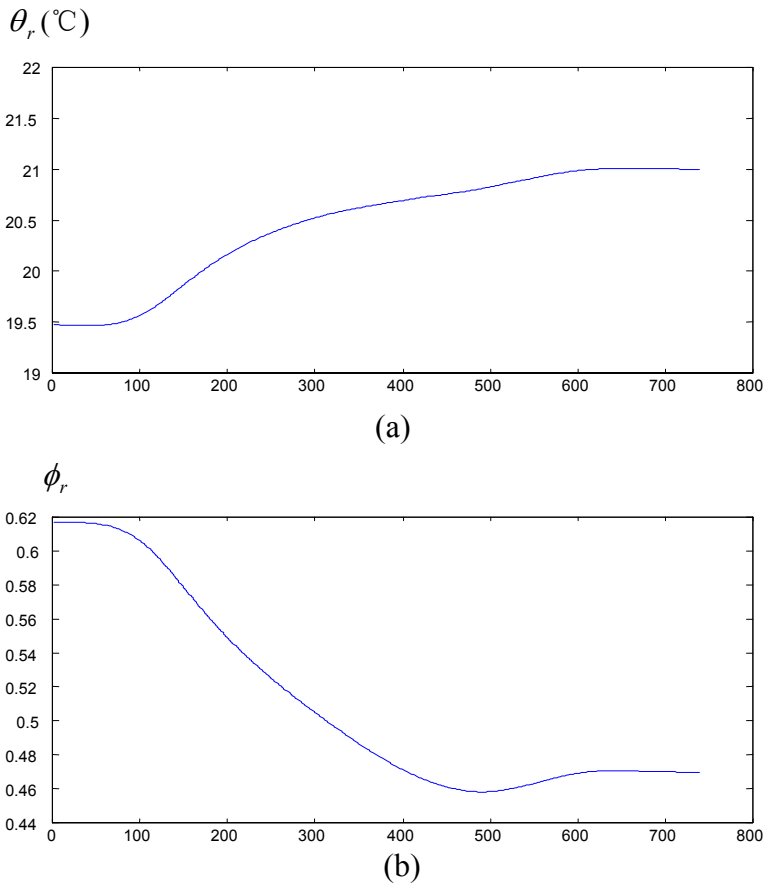

Figure 3-9 Room temperature and RH response to a step change in supply airflow rate

In another experiment, the responses of the room temperature and RH to a step change in supply airflow rate were observed. The fan speed was reduced from 2100 to 900 rpm while the chilled water valve opening was kept at 100% opening. From the responses shown in Fig. 3-9, it can be seen that the room temperature rises to 21℃ with the decreasing supply airflow rate. At the same time, the room RH decreases to 47%. This implies that a lower airflow rate produces smaller sensible cooling capacity and greater latent cooling capacity.

3.4 Concluding Remarks

From the theoretical analyses, it is shown that it is feasible to control both the room temperature and RH simultaneously by varying the supply airflow rate and the chilled water flow rate. The experimental results are in agreement with the theoretical analyses. Some system parameters need to be determined in developing the model of the air-conditioning system. However, some of the parameters are difficult to get and they vary with the different operating conditions. Non-linearity is also present in VAV systems. From the initial experiments, it is seen that the response rate of room temperature and RH is different when the chilled water flow rate or airflow rate is changed. The different response rates suggest that different sampling intervals should be used for temperature and RH control.

CHAPTER 4
FUZZY LOGIC CONTROL SYSTEM

In Chapter 3, it was shown that it is feasible to control both room temperature and RH by varying the supply airflow rate and the chilled water flow rate. Two control strategies are explored here. One strategy is to control room temperature by varying the supply air fan speed and room RH by varying the chilled water valve opening. This strategy will be referred to in this work as control Strategy 1. The other strategy is to control room temperature by varying the chilled water valve opening and room RH by varying the supply air fan speed. This strategy will be referred to as Strategy 2. However, Strategy 1 was found to be successful while Strategy 2 failed in experiments.

The objective of the control system is to regulate the room temperature and RH to their desired values, θ_{set} and ϕ_{set}. The block diagram of the air-conditioning control system is a simple closed loop system as shown in Fig. 4-1.

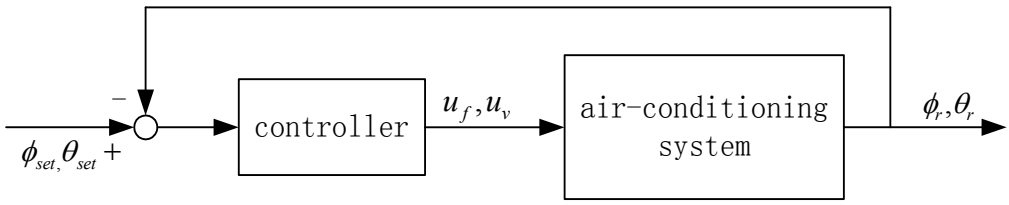

Figure 4-1 Air-conditioning control system

The controller is designed to provide the proper supply air fan speeds and chilled water valve openings to the air-conditioning plant, so that the room temperature and RH are maintained at their desired set points.

4.1 Fuzzy Controller Design

The controller is designed using fuzzy logic. Inputs to the controller are the set point of room temperature θ_{set} and set point of room RH ϕ_{set}, the actual room temperature θ_r and RH ϕ_r. The outputs are the supply air fan speed u_f and the chilled water valve opening u_v. Control Strategy 1 is implemented. The control strategy used can be expressed by the following linguistic rules:

If room temperature is higher than the set point, then increase the supply air fan speed.

If room RH is higher than the set point, then increase the chilled water valve opening.

4.1.1 Structure of the Fuzzy Logic Controller

The air-conditioning system is a MIMO process. It is difficult to directly design a MIMO fuzzy controller because too many rules will be involved. At the same time, there is always not enough expert knowledge available to set the fuzzy rules. One easier approach is to decouple the MIMO controller into several SISO controllers. The fuzzy controller is then composed of a fuzzy temperature sub-controller and a fuzzy relative humidity sub-controller, as shown in Fig. 4-2.

A two-dimensional fuzzy controller is adopted, with the error of the controlled variable, E, and its rate of change, $\dot{E}$, being the inputs. More dimensions will make the controller too complicated.

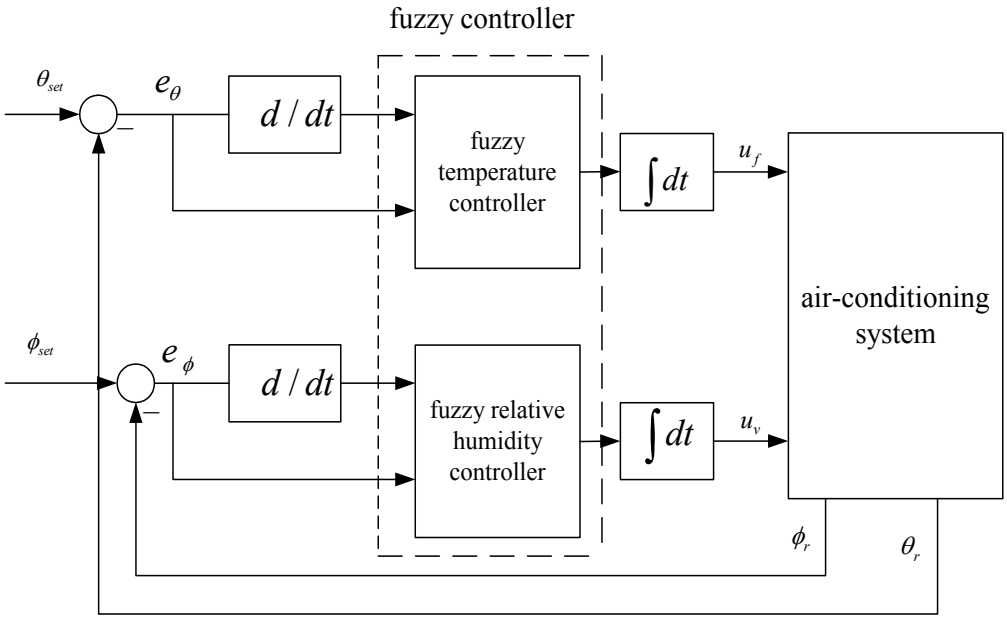

Figure 4-2 Structure of the fuzzy control system

To control the room temperature, the controller first reads the room temperature θ_r and reference set point θ_{set}. The temperature error e_θ and its rate of change $\dot{e}_\theta$ are then computed and used as the inputs to the fuzzy temperature controller.

$$e_\theta = \theta_{set} - \theta_{rk} \tag{4-1}$$

$$\dot{e}_\theta = \theta_{r(k-1)} - \theta_{rk} \tag{4-2}$$

where θ_{rk} is the measured room temperature at the kth sampling instant.

The required change of the supply fan speed Δu_f, which is the output of the fuzzy temperature controller, is then deduced from fuzzy inference

$$\Delta u_f = f(e_\theta, \dot{e}_\theta) \tag{4-3}$$

In the same way, to control the room RH, the controller first reads the room RH ϕ_r and reference point ϕ_{set}. The RH error e_ϕ and its rate of change $\dot{e}_\phi$ are then computed and used as inputs to the fuzzy relative humidity controller.

$$e_\phi = \phi_{set} - \phi_{rk} \tag{4-4}$$

$$\dot{e}_\phi = \phi_{r(k-1)} - \phi_{rk} \tag{4-5}$$

where ϕ_{rk} is the room RH at the kth sampling instant.

The required change of the chilled water valve opening Δu_v, which is the output of the fuzzy relative humidity controller, is then deduced from fuzzy inference

$$\Delta u_v = f(e_\phi, \dot{e}_\phi) \tag{4-6}$$

4.1.2 Membership Function

In the fuzzy controller, the If-Then rules are written using fuzzy sets, which are characterized by membership functions. Seven fuzzy sets are defined for each input variable. They are PL (positive large), PM (positive medium), PS (positive small), ZO (zero), NS (negative small), NM (negative medium) and NL (negative large).

Triangular membership functions are used here because they are simple and have been proven to be sufficient in many applications. Fig. 4-3 shows the antecedent membership functions. They are used for the temperature error e_θ and its rate of change $\dot{e}_\theta$, and for the RH error e_ϕ and its rate of change $\dot{e}_\phi$.

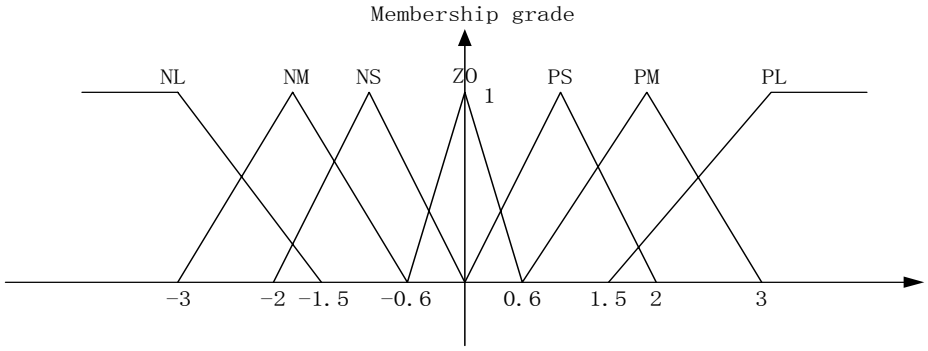

Figure 4-3 Membership functions definition

The membership functions, μ being membership grade, are expressed as:

$$1.\ \text{NL:}\ \mu_1 = \begin{cases} 0, & x = [-1.5, +\infty] \\ 1 - |x+3|/1.5, & x = [-3, -1.5] \\ 1, & x = [-\infty, -3] \end{cases} \tag{4-7}$$

$$2.\ \text{NM:}\ \mu_2 = \begin{cases} 1 - |x+1.8|/1.2, & x \in [-3, -0.6] \\ \\ 0, & \text{otherwise} \end{cases} \tag{4-8}$$

$$3.\ \text{NS:}\ \mu_3 = \begin{cases} 1 - |x+1|, & x \in [-2, 0] \\ \\ 0, & \text{otherwise} \end{cases} \tag{4-9}$$

$$4.\ \text{ZO:}\ \mu_4 = \begin{cases} 1 - |x|/0.6, & x \in [-0.6, 0.6] \\ \\ 0, & \text{otherwise} \end{cases} \tag{4-10}$$

$$5.\ \text{PS:}\ \mu_5 = \begin{cases} 1 - |x-1|, & x \in [0, 2] \\ \\ 0, & \text{otherwise} \end{cases} \tag{4-11}$$

$$\text{6. PM: } \mu_6 = \begin{cases} 1-|x-1.8|/1.2, & x \in [0.6,3] \\ \\ 0, & \text{otherwise} \end{cases} \tag{4-12}$$

$$\text{7. PL: } \mu_7 = \begin{cases} 0, & x = [-\infty,1.5] \\ 1-|x-3|/1.5, & x = [1.5,3] \\ 1, & x = [3,+\infty] \end{cases} \tag{4-13}$$

Membership functions must adequately cover the input range. The shape of membership functions has effect on the performance of the fuzzy controller. Higher resolution and sensitivity are obtained if the sides of the triangles have steeper slopes. On the other hand, gentler slopes lead to a smoother control action and greater stability. The distribution of membership functions need also be taken into consideration in their definition. In the neighborhood of zero, a high-resolution function is chosen. Low-resolution membership functions are defined in areas far from zero to achieve higher robustness and stability.

Because these fuzzy sets are defined on the universe of discourse $[-3,+3]$, the actual crisp input must be translated into this universe. The actual input values, e_θ, $\dot{e}_\theta$, e_ϕ and $\dot{e}_\phi$, must first be scaled to E_θ, $\dot{E}_\theta$, E_ϕ, $\dot{E}_\phi$ by the use of the scaling factors.

$$E_\theta = e_\theta * K_{E_\theta} \tag{4-14}$$

$$\dot{E}_\theta = \dot{e}_\theta * K_{\dot{E}_\theta} \tag{4-15}$$

$$E_\phi = e_\phi * K_{E_\phi} \tag{4-16}$$

$$\dot{E}_\phi = \dot{e}_\phi * K_{\dot{E}_\phi} \tag{4-17}$$

The values after translation are still crisp. They are therefore fuzzified into fuzzy values according to the membership functions.

4.1.3 Fuzzy Inference

The zero-order T-S fuzzy rules are used

$$\text{If } E \text{ is } A_i \text{ and } \dot{E} \text{ is } B_j, \text{ then } \Delta F = C_{ij}. \qquad 4\sim1$$

where, A_i and B_j are fuzzy sets defined for E and $\dot{E}$ respectively. The output C_{ij} is a crisply defined constant.

The advantages of using this type of rules are simple calculation and easy tuning (Funakoshi and Matsuo, 1995). Taking the variables error and rate of its change as the controller inputs is similar to the proportional and derivative term in conventional crisp controllers. The consequent of the rule, C_{ij}, is the change in control action. The output of the fuzzy controller is the control signal increment to be applied to the control device. By this means, integral action is incorporated into the controller. The fuzzy controller is thus somewhat like a nonlinear PID controller.

The $Max-Min$ inference method is employed and the weighted mean method (WMM) is used in defuzzification. Example of processing two sets of combination of E and $\dot{E}$ according to the Rule 4~1 is shown in Fig. 4-4. Each combination will produce a crisp value of the control action according to a table of fuzzy control rules. These are shown as C_{11} and C_{22} in this figure.

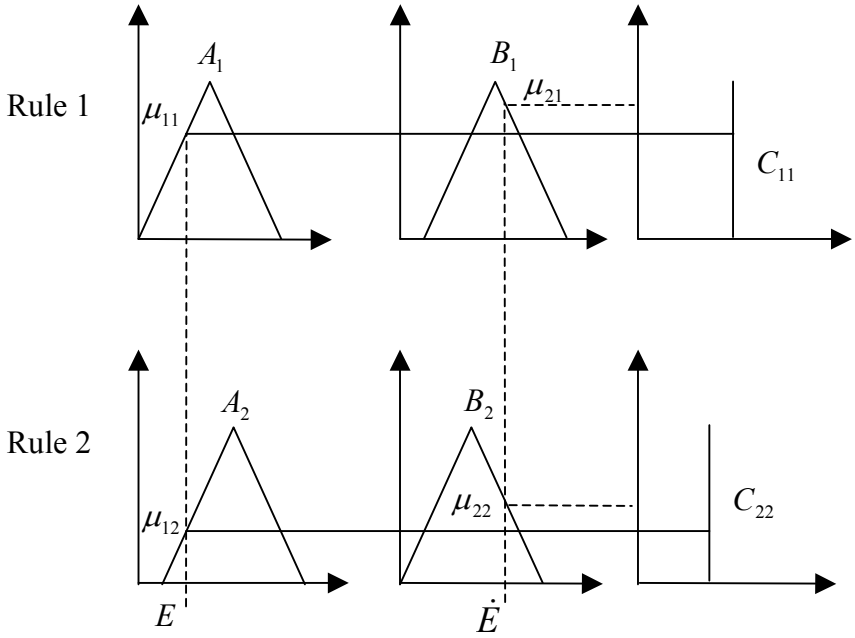

Figure 4-4 Fuzzy inference diagram

In the first step, E and $\dot{E}$ are resolved into fuzzy linguistic sets. After fuzzification, E is "A_1" to degree μ_{11} and "A_2" to degree μ_{12}. $\dot{E}$ is "B_1" to degree μ_{21} and "B_2" to degree μ_{22}.

The *Min* operator is used to perform the AND operation for the Rule 4~1 to give the weighted mean to the control action resulting from the applications of the rule to each set of combination. In the example in Fig. 4-4, these are

$$\varepsilon_{11} = \min(\mu_{11}, \mu_{21}) \tag{4-18}$$

$$\varepsilon_{22} = \min(\mu_{12}, \mu_{22}) \tag{4-19}$$

Finally, a single output from the fuzzy controller is calculated using the weighted mean method as:

$$\Delta P = \frac{\varepsilon_{11} C_{11} + \varepsilon_{22} C_{22}}{\varepsilon_{11} + \varepsilon_{22}} \qquad (4\text{-}20)$$

4.1.4 Fuzzy Rules

The fuzzy control rules are generated referring to various publications (Funakoshi and Matsuo, 1995). These rules can be adjusted according to the performance trajectory on the linguistic plane (Huang and Nelson, 1994). The control rules, consisting of percentage changes, C_{ij}, to the control action, are listed in Table 4-1. These are used for the fuzzy controller for both temperature and RH. There are altogether 49 numbers as seven fuzzy sets are defined for each of E and $\dot{E}$ in the controller design. From the table it can be seen that the largest positive control action occurs in the upper left cell when both E and $\dot{E}$ are NL. It is logical, for example, to increase the supply air fan speed by the largest amount if the room temperature is much higher than the set point and it is still increasing rapidly.

Table 4-1 Fuzzy control rules

E \ $\dot{E}$	NL	NM	NS	ZO	PS	PM	PL
NL	30	22	16	10	6	2	-4
NM	24	18	12	6	2	-4	-8
NS	20	12	6	2	-2	-8	-14
ZO	17	10	4	0	-4	-10	-17
PS	14	8	2	-2	-6	-12	-20
PM	8	4	-2	-6	-12	-18	-24
PL	4	-2	-6	-10	-16	-22	-30

To interpret the table, take for example the upper leftmost rule,

> *If the room temperature error is NL and its rate of change is NL, then increase the supply air fan speed by 30%.*

Or,

If the room RH error is NL and its rate of change is NL, then increase the chilled water valve opening by 30%.

The output of the fuzzy controller, which is the weighted mean of all the resulting control actions given by each fuzzy control rule is then generated as:

$$\Delta P = \frac{\sum \varepsilon_{ij} C_{ij}}{\sum \varepsilon_{ij}} \tag{4-21}$$

where $\varepsilon_{ij} = \min(\mu(A_i), \mu(B_j))$ as discussed in the previous section, and C_{ij} is the crisp control value from fuzzy control rules in Table 4-1.

The change in output control action, Δu , is then computed from the following equation:

$$\Delta u = K_u u(k) \Delta P \tag{4-22}$$

where K_u is a control gain constant and $u(k)$ is the current value of the control action. The control action given at the next sampling instant is then given as:

$$u(k+1) = u(k) + \Delta u \tag{4-23}$$

4.2 Experimental Results

4.2.1 Sampling Interval Determination

It is important to select a suitable sampling interval in a computer control system. A sampling interval that is much larger than the time constant of the system yields data

with insufficient information about the dynamics. On the other hand, a smaller sampling interval is prone to noise interference.

The sampling interval can be determined based on the open-loop system response. The room temperature and RH responses to a step change in fan speed and chilled water valve opening has earlier been investigated in Chapter 3. Denoting T_{st} as the process settling time, the sampling time can be chosen in the range of (Zhu, 2001)

$$T = \frac{T_{st}}{20} \text{ to } \frac{T_{st}}{100} \tag{4-24}$$

Referring to Fig. 3-8 (b), which gives the room RH response to a step change in the chilled water valve opening, the settling time is 1500 seconds. Thus, a sampling interval T_{ϕ} of 50 seconds is used for relative humidity control. Referring to Fig. 3-9 (a) for the room temperature response to a step change in the fan speed, the settling time is 5000 seconds. A sampling interval T_{θ} of 4 minutes is used for temperature control. While the sampling periods T_{θ} and T_{ϕ} are used for control, that is, update of the control action, in the experiments described in the following sections, both the temperature and RH were sampled at 10 seconds intervals for record purpose.

4.2.2 Experiments

The designed fuzzy controller was implemented on the air-conditioning system to determine its performance.

The room temperature and RH were set at 25℃ and 60% respectively. In order to bring down the room temperature quickly, the fan speed was set at a high speed (35Hz, 2100

rpm) and the chilled water valve opening was set at 100% at system start-up. After the room temperature dropped to 25.5℃, the fuzzy controller started to work. The input scaling factors used were $K_{E_\theta} = 6$, $K_{\dot{E}_\theta} = 30$, $K_{E_\phi} = 300$, $K_{\dot{E}_\phi} = 150$. It can be seen from Fig. 4-5 that the room temperature response is satisfactory, but oscillations persist for a long time around the set point in the room RH response. From this figure, it is observed that the supply air fan speed operated at a low speed after the room temperature has reached its set point.

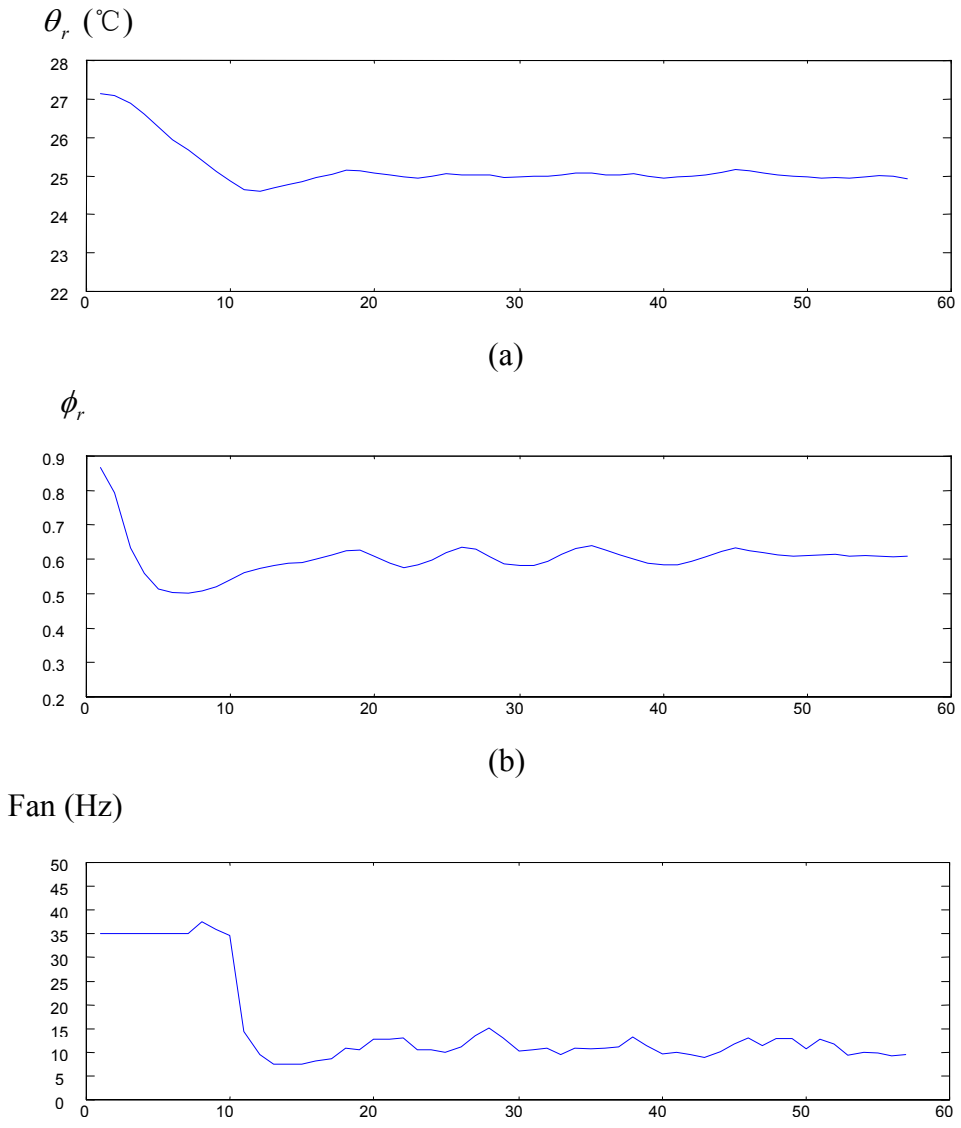

Figure 4-5 Fuzzy controller test result 1

In order to eliminate the RH oscillations, the input scaling factor K_{E_ϕ} was reduced to $K_{E_\phi} = 100$ in the subsequent experiment. From Fig. 4-6, it can be seen that RH becomes more stable after the reduction.

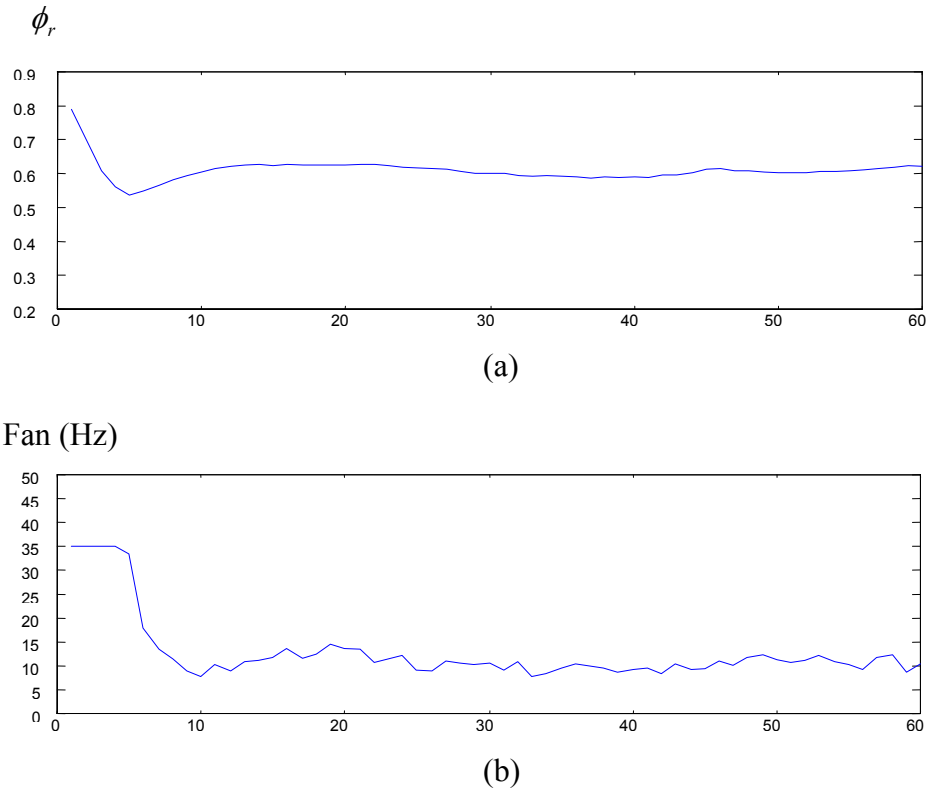

Figure 4-6 Fuzzy controller test result 2

In the following experiments, fuzzy control was implemented from system start-up. As shown in Fig. 4-7 (b), the RH oscillates continuously. Reducing the control gain at the output of the humidity controller (refer to Eq.4-22) from $K_{u_\phi} = 1$ to $K_{u_\phi} = 0.5$ results in the RH response becoming more stable with a very small error, as shown in Fig. 4-7(c).

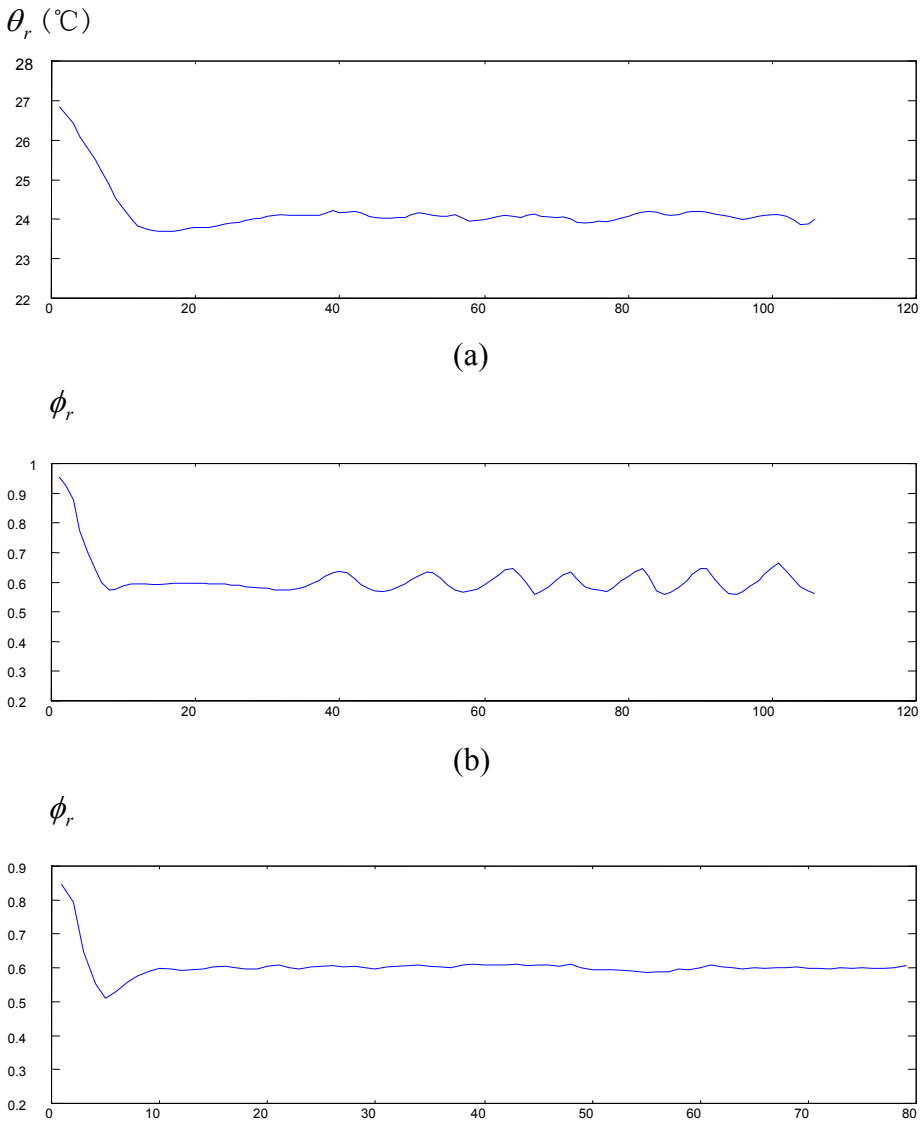

Figure 4-7 Fuzzy controller test result 3

Fig. 4-8 shows the system response when there is a change in the set point of the room temperature. The room temperature set point is changed from 25℃ to 24℃ at time t=50min. There was only a small deviation of RH from its set point and the room RH returned to the steady state after only a short period. It demonstrates the favorable tracking ability of the fuzzy controller.

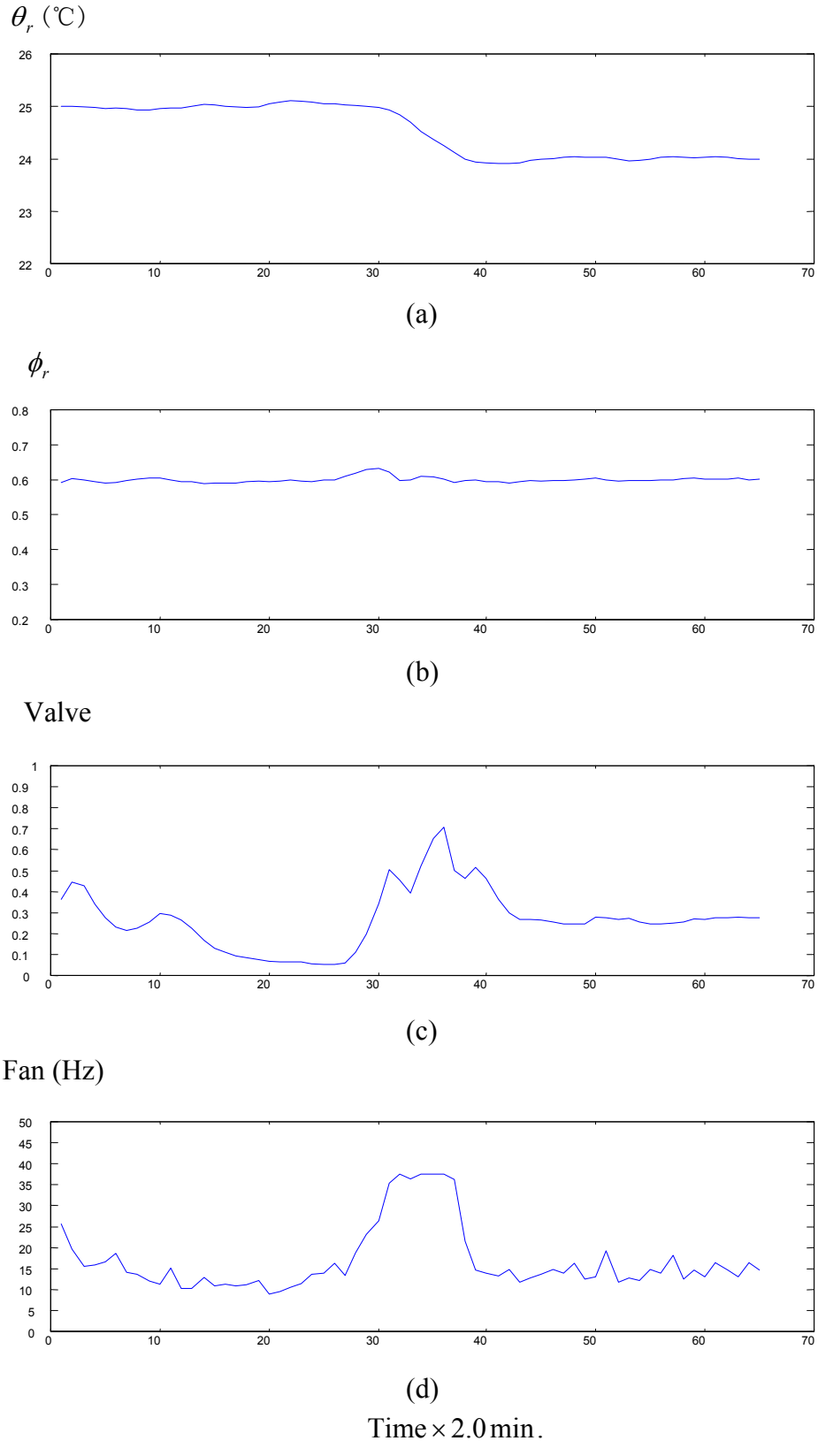

Figure 4-8 Room temperature and RH response
to a step change in set point of temperature

The responses of room temperature and RH were next tested in response to a change in the heat load in the room. In the experiment, the setting of the heater thermostat was changed to a higher temperature at time t=60min. From Fig. 4-9, it is seen that the room temperature has a small deviation from the set point but returns rapidly. The RH is maintained at its set point value without any deviation. The result shows the controller's robustness to a sensible heat load disturbance.

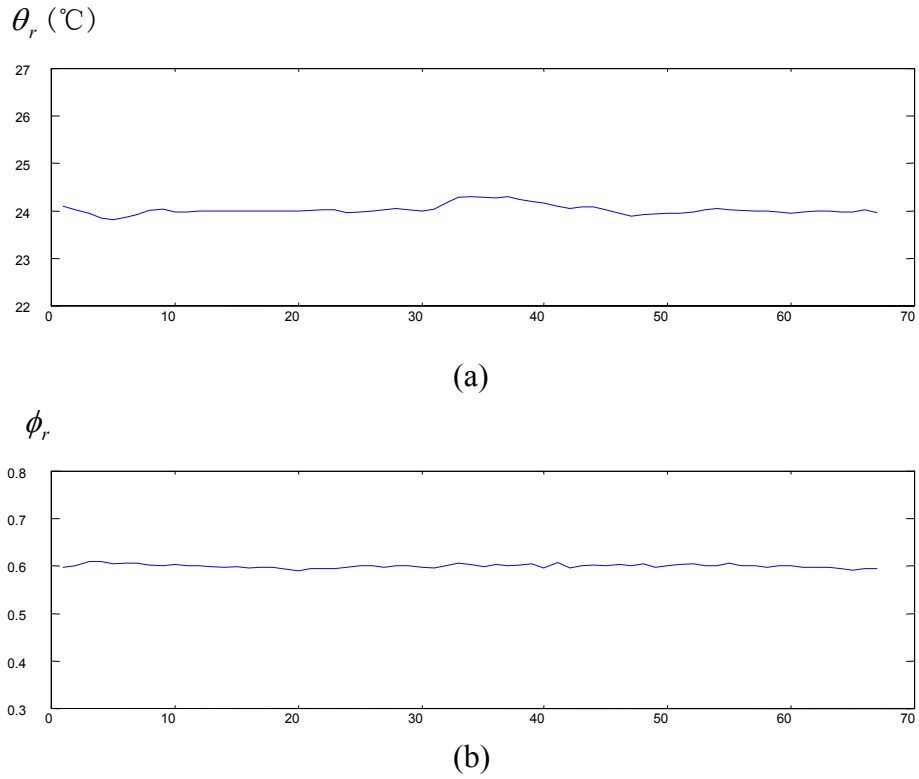

Figure 4-9 Room temperature and RH response to change in heat load

4.3 Concluding Remarks

The other control strategy of controlling the room temperature by varying the chilled water valve and RH by varying the supply fan speed was also investigated. This control strategy was not successful in the experiments. Referring to Fig. 3-8 and Fig. 3-9, it can be inferred that changes in sensible and latent capacity due to percentage

changes in the fan speed are greater than corresponding changes due to same percentage changes in the chilled water valve opening. Since sensible load is generally greater than latent load, and changes in sensible load are greater than changes in latent load, it is more logical to control the room temperature by controlling the fan speed and to control room RH by controlling the chilled water valve opening.

Two separate fuzzy sub-controllers were used to control the temperature and RH so that the difficulty of designing a multi-input multi-output controller is avoided. Different sampling intervals should be adopted for temperature and RH control because of their different time constants. This is to achieve good dynamic control for both while reducing the effect of noise.

Experiments were conducted to investigate the performance of the fuzzy controller. From these experiments, it is shown that the fuzzy controller can successfully track the room temperature and RH set points. The fuzzy controller was insensitive to the coupling of the temperature and RH. Even if the set point of one variable was changed, the other variable kept stable. Experimental results also showed the good disturbance rejection capability of the fuzzy controller.

The input scaling factors and output gains used can significantly influence the fuzzy controller performance. Larger scaling factors and gains can increase the speed of the control action, but these can lead to oscillations and overshoots. Compared with the input variable scaling factors, the control gains at the output have a more significant effect.

CHAPTER 5
FUZZY NEURAL NETWORK CONTROLLER

In Chapter 4, it was shown that fuzzy logic could be successfully applied to room temperature and RH control. However, the fuzzy logic controller is built on linguistic rules given by human experts. Sometimes, there is not enough expert knowledge available or the initial fuzzy rules may even be incorrect. The fuzzy rules adopted for one system may not be applicable to other system. In these conditions, tuning of fuzzy controller is necessary (Huang and Nelson, 1999). However, tuning of fuzzy systems is not a straightforward task, e.g., how to arrive at the optimal membership functions and the fuzzy rules.

Neural networks have the ability of self-learning. This chapter presents a self-tuning fuzzy controller integrating fuzzy logic with neural networks. The fuzzy controller is built in a neural network structure, and the parameters of the fuzzy controller can be treated as the connecting weights in the neural network. By this means, tuning of the fuzzy system is achieved through training of the neural network.

5.1 Fuzzy Neural Networks

The fuzzy logic system can be constructed with a multi-layer feed-forward neural network (Chen and Teng, 1995). A schematic diagram of a fuzzy neural network (FNN) architecture is shown in Fig. 5-1. Two input variables and one output variable are assumed in this figure. The network consists of four layers. There are two inputs, x_1 and x_2, to the neural network and the output of the neural network is y. Nodes in the

1st layer transmit input variables to the next layer directly, with unity connecting weights. Nodes in Layer 2 are membership nodes that act like membership functions. Each membership node is responsible for mapping an input linguistic variable into a possible distribution for that variable. Each node in the 3rd layer is used to perform matching of a fuzzy logic rule. Taken together, all nodes in this layer form the fuzzy rule base. The node in the last layer gives the final output.

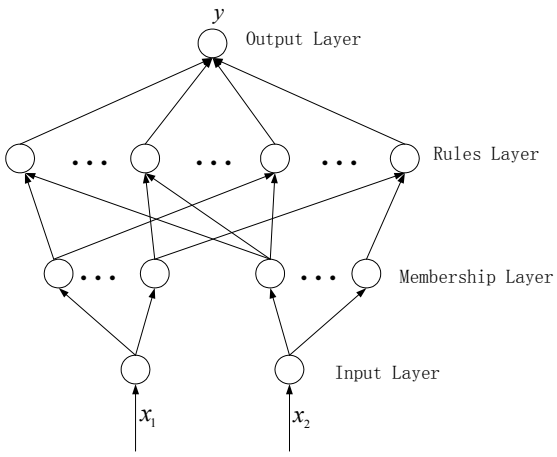

Figure 5-1 Fuzzy neural networks

In order to ensure differentiability, the *Sum-Product* inference method is adopted instead of the *Max-Min* method and weighted sum is used in defuzzification. Define α_{ij} as the firing strength of a rule and w_{ij} as the consequent of the rule, the output y^* of the output node is then obtained from the weighted sum of its inputs. The inference is expressed as:

$$\text{If } x_1 \text{ is } A_{1i} \text{ and } x_2 \text{ is } A_{2j}, \text{ then } y = w_{ij}. \qquad 5\sim1$$

$$y^* = \sum \alpha_{ij} w_{ij},\ \alpha_{ij} = \mu_{A_{1i}}(x_1)\mu_{A_{2j}}(x_2)$$

where $\mu_{A_{1i}}(x_1)$ and $\mu_{A_{2j}}(x_2)$ are membership grade of x_1 and x_2 to fuzzy sets, A_{1i} and A_{2j}, respectively.

5.1.1 Nodes Operation

Assuming seven fuzzy sets are defined for each linguistic variable, the function of nodes in each layer is described in the following section.

Layer 1: input layer

There are two nodes in this layer. Each of these just transmits an input variable to the second layer. The outputs of this layer are the same as the inputs to the neural network, i.e. x_i, $i = 1,2$.

Layer 2: membership layer

Because seven membership functions are defined for each input variable, there are 14 nodes in this layer. Each of these performs a membership function. Triangular membership functions are used. These are schematically shown in Fig. 5-2.

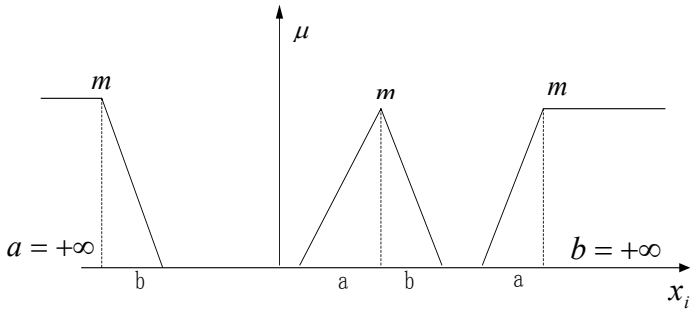

Figure 5-2 Membership function

There are three adjustable parameters, m, a and b, in this kind of membership functions. m, a and b correspond to the center, the left spread, and the right spread of the triangle, respectively. As shown in this figure, the trapezoid can also be regarded as a special triangle. Referring to Fig. 5-2, the outputs of the nodes in Layer 2 are given as:

$$\sigma_{ij} = \begin{cases} 1 - \left| x_i - m_{ij} \right| / b_{ij}, & x_i \in \left[m_{ij}, m_{ij} + b_{ij} \right] \\ 1 - \left| x_i - m_{ij} \right| / a_{ij}, & x_i \in \left[m_{ij} - a_{ij}, m_{ij} \right] \\ 0, & \text{otherwise} \end{cases} \quad \text{for} \begin{matrix} i = 1,2 \\ j = 1,2,...,7 \end{matrix} \tag{5-1}$$

where the subscript *ij* corresponds the jth membership function of the ith input variable x_i.

Layer 3: rule layer

The nodes in this layer implement the antecedent matching. There are 49 nodes in this layer because seven membership functions are defined for each input variable. Here, the matching is performed using the PRODUCT operation. Thus, the outputs of the nodes are given by:

$$\omega_{ij} = \sigma_{1i} \sigma_{2j}, \quad \text{for} \begin{matrix} i = 1,2...,7 \\ j = 1,2...,7 \end{matrix} \tag{5-2}$$

Layer 4: output layer

The overall output of the neural networks is the weighted sum of consequents of all the 49 fuzzy rules. The output of the only one node is then defined by

$$y = \sum_{i=1}^{7} \sum_{j=1}^{7} w_{ij} \omega_{ij}, \quad \text{for} \begin{matrix} i = 1,2...,7 \\ j = 1,2...,7 \end{matrix} \tag{5-3}$$

where w_{ij} is the consequent of the fuzzy rule.

By modifying the centers and spreads of Layer 2 and the connecting weights of Layer 4, the membership functions can be adjusted and all the consequents of the fuzzy rules can be identified respectively.

5.1.2 Training of FNN

The adjustment of the parameters in the proposed FNN is achieved through training of the neural network. The supervised learning law is used to train the FNN. The basis of this algorithm is steepest gradient descent. By recursive application of the chain rule, the error term for each layer is calculated and the adaptation of the weights is given. In the following, the training law for each layer is derived in the feedbackward direction.

The cost function to be minimized is:

$$E = \frac{1}{2}(y_d - y)^2 = \frac{1}{2}e^2 \tag{5-4}$$

where y_d is the desired output and y is the actual output of the fuzzy neural network. The error signal is be propagated consecutively from Layer 4 to Layer 1. Here, δ is the local gradient.

Layer 4:

$$\delta^4 = \frac{-\partial E}{\partial y} = y_d - y = e \tag{5-5}$$

Therefore the weight w_{ij} is updated by the amount:

$$\Delta w_{ij} = \frac{-\partial E}{\partial w_{ij}} = \frac{-\partial E}{\partial y}\frac{\partial y}{\partial w_{ij}} = \delta^4 \omega_{ij} \qquad \text{for} \begin{matrix} i = 1,2,...,7 \\ j = 1,2,...,7 \end{matrix} \tag{5-6}$$

Layer 3: Since the weights in this layer are unity, none of them is to be modified. The error term is only calculated and propagated.

$$\delta_{ij}^3 = \frac{-\partial E}{\partial \omega_{ij}} = \frac{-\partial E}{\partial y}\frac{\partial y}{\partial \omega_{ij}} = \delta^4 w_{ij} \qquad \begin{matrix} i = 1,2,...,7 \\ j = 1,2,...,7 \end{matrix} \tag{5-7}$$

Layer 2: The multiplication operation is done in this layer. m and a, b are adapted as follows:

$$\delta_{ij}^2 = \frac{-\partial E}{\partial \sigma_{ij}} \tag{5-8}$$

$$\delta_{1j}^2 = \sum_{k=1}^{7} \delta_{jk}^3 \sigma_{2k} \qquad j = 1,2,...,7 \tag{5-9}$$

$$\delta_{2j}^2 = \sum_{k=1}^{7} \delta_{kj}^3 \sigma_{1k} \qquad j = 1,2,...,7 \tag{5-10}$$

The modification of the center, the left spread and the right spread of the triangular membership functions can then be computed by:

$$\Delta m_{ij} = \frac{-\partial E}{\partial m_{ij}} = \frac{-\partial E}{\partial \sigma_{ij}} \frac{\partial \sigma_{ij}}{\partial m_{ij}} = \begin{cases} \delta_{ij}^2 (-\frac{1}{a_{ij}}), & x_i \in [m_{ij} - a_{ij}, m_{ij}] \\ \delta_{ij}^2 (\frac{1}{b_{ij}}), & x_i \in [m_{ij}, m_{ij} + b_{ij}] \end{cases} \tag{5-11}$$

$$\Delta a_{ij} = \frac{-\partial E}{\partial a_{ij}} = \frac{-\partial E}{\partial \sigma_{ij}} \frac{\partial \sigma_{ij}}{\partial a_{ij}} = \delta_{ij}^2 \left[\frac{(m_{ij} - x_i)}{a_{ij}^{\ 2}} \right], x_i \in [m_{ij} - a_{ij}, m_{ij}] \tag{5-12}$$

$$\Delta b_{ij} = \frac{-\partial E}{\partial b_{ij}} = \frac{-\partial E}{\partial \sigma_{ij}} \frac{\partial \sigma_{ij}}{\partial b_{ij}} = \delta_{ij}^2 \left[\frac{(x_i - m_{ij})}{b_{ij}^{\ 2}} \right], x_i \in [m_{ij}, m_{ij} + b_{ij}] \tag{5-13}$$

After getting the adaptations of these adjustable parameters, their new values are decided from the following four equations.

$$w_k(n+1) = w_k(n) + \eta_1 \Delta w_k(n) \tag{5-14}$$

$$m_{ij}(n+1) = m_{ij}(n) + \eta_2 \Delta m_{ij}(n) \tag{5-15}$$

$$a_{ij}(n+1) = a_{ij}(n) + \eta_3 \Delta a_{ij}(n) \tag{5-16}$$

$$b_{ij}(n+1) = b_{ij}(n) + \eta_4 \Delta b_{ij}(n) \qquad (5\text{-}17)$$

where η is the learning rate.

5.2 Control System Structure

Model reference adaptive control (MRAC) structure is used to design the control system (Narendra and Parthasarathy, 1990). MRAC is an adaptive control scheme, with a reference model specifying the desired closed loop response of the control system. The controller parameters are tuned online to adapt to variations in the controlled plant characteristics making use of the output error between the reference model and the actual system output.

5.2.1 Control Scheme

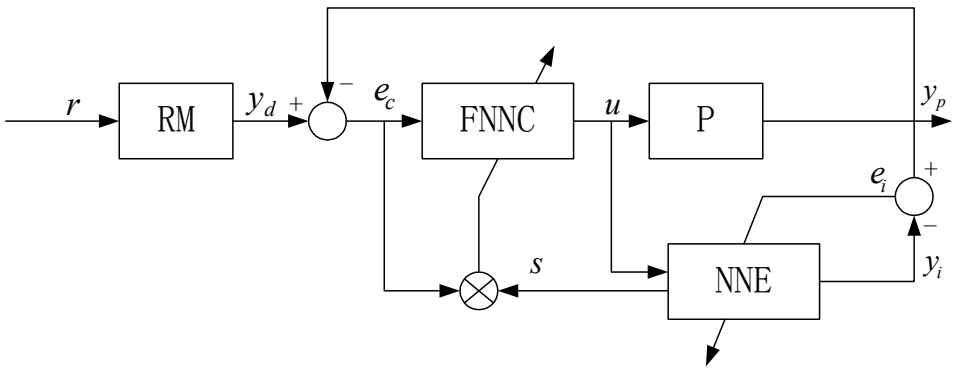

Figure 5-3 Model reference control scheme using fuzzy neural network

The control structure is shown in Fig. 5-3. The reference model (RM) gives the desired output y_d for the control system. A feedback controller is designed to produce system input u so that the actual output, y_p, of the system P will track the desired output of the reference model. A fuzzy neural network (FNNC) is used, so the control system can reason and learn by experience and adapt to changes in plant parameters.

The controlled plant is an air-conditioning system in the work with the room temperature θ_r and RH ϕ_r being the controlled variables. The RM prescribes the desired room temperature and RH. The FNNC provides actuating actions to the air-conditioning plant in order to achieve this.

Similar to the fuzzy controller design in Chapter 4, the FNNC is also composed of two separate fuzzy neural networks. One fuzzy neural network is used for the control of room temperature, the other for room RH. The inputs to each controller are the controlled variable error and its rate of change.

5.2.2 Training of FNNC

From Fig. 5-3, it can be seen that the output of FNNC is the control signal u imposed on the system. The cost function used for the FNNC is:

$$E_c = \frac{1}{2} e_c^{\,2} = \frac{1}{2}\left[y_d(t) - y_p(t)\right]^2 \tag{5-18}$$

The learning law discussed in Section 5.1.2 cannot be used directly. It can be solved by changing the computation of δ^4 because the error term is back propagated.

$$\delta^4 = \frac{-\partial E_c}{\partial y} = \frac{-\partial E_c}{\partial e_c}\frac{\partial e_c}{\partial y_p}\frac{\partial y_p}{\partial u}\frac{\partial u}{\partial y}$$

$$= e_c \frac{\partial y_p}{\partial u} \tag{5-19}$$

where $s = \dfrac{\partial y_p}{\partial u}$ is the plant sensitivity, which represents the change of the system output to a change in the system input. In order to get the plant sensitivity, one neural network emulator (NNE) is added to the control system. This neural network is trained

to predict the plant state y_i, with the actual value of the state of the plant y_p used as the desired response.

5.3 Neural Network Emulator

The NNE is designed to identify the dynamic characteristics of the air-conditioning system. It predicts the room temperature and RH in advance.

5.3.1 Structure of NNE

The performance of neural networks is determined by selection of inputs to the network and internal network architecture (Nørgaard, 2000). In the first step, the inputs of NNE must be properly defined. From equations in Chapter 3, it is clear that the room temperature θ_r and RH ϕ_r are nonlinear functions of the supply air temperature θ_s, supply air RH ϕ_s, and supply airflow rate m_a if the outdoor temperature and humidity and indoor heat load are considered as disturbances. The supply air temperature θ_s and supply air RH ϕ_s are also dependent on the supply airflow rate m_a and the chilled water flow rate m_w, which corresponds to the supply air fan speed and chilled water valve opening respectively. Therefore, the system status can be characterized by four variables, θ_r, ϕ_r, θ_s, ϕ_s and two actuating signals, the supply air fan speed u_f and the chilled water valve opening u_v.

Cybenko (1989) proposed that all continuous functions could be approximated to any desired accuracy, in terms of the uniform norm, with a network of one hidden layer of sigmoid hidden nodes and a layer of linear output units. A neural network with one

hidden layer is employed in the work. The hidden layer neurons employ the sigmoid function:

$$f(x) = \frac{1}{1 - e^{-x}} \tag{5-20}$$

The values of the input variables at the present sampling instant k and the previous sampling instant $k-1$ are inputs to the NNE. The outputs of the neural network are the θ_r and ϕ_r at the next sampling instant $k+1$.

5.3.2 Training Data Generation

The neural network emulator needs enough training to accurately emulate the air-conditioning system. The error between the actual data and the predicted data is used to train the network. The actual data can be acquired from the plant model or from experiments. Because an accurate mathematical model of the air-conditioning system is difficult to obtain, actual measured input-output data are used to train the neural network.

For proper operation of the NNE, measured input-output training data used must adequately cover the whole operating region of the system. The swept sine function is used as the excitation function to generate training examples (Xi et al., 1998).

$$u(t) = 0.5 + 0.5\sin\left[(\omega_0 + Rt)t\right] \tag{5-21}$$

This is shown in Fig. 5-4. The supply air fan speed u_f and chilled water valve opening u_v were varied using the swept sine signal. Some experiments were conducted to generate the training examples. In the experiments, θ_r, ϕ_r, θ_s, ϕ_s, u_f and u_v were monitored and recorded.

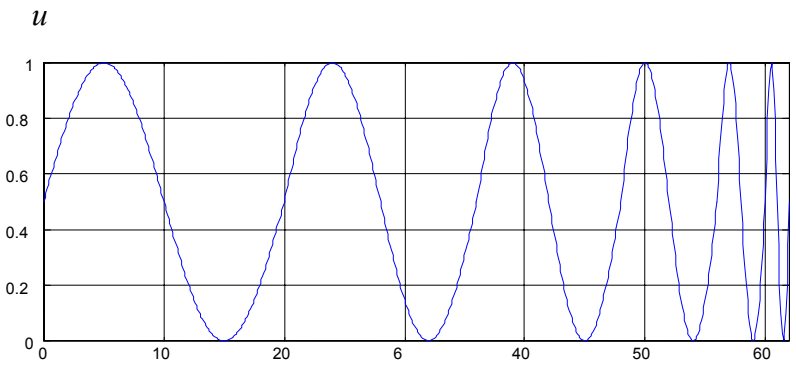

Figure 5-4 Swept sine actuating signal

5.3.3 Training and Validation

In order that a model is meaningful for control purposes, the sampling interval for model development should be the same as for the control application. For this reason, different sampling intervals, 4min and 50sec, were used for the room temperature and RH. Therefore, the room temperature and RH are separately predicted during the experiments to generate training data.

$$\theta_r(k+1) = f_1[\theta_r(k),\theta_r(k-1),\phi_r(k),\phi_r(k-1),\theta_s(k),\theta_s(k-1),\\ \phi_s(k),\phi_s(k-1),u_f(k),u_f(k-1),u_v(k),u_v(k-1)] \tag{5-22}$$

$$\phi_r(k+1) = f_2[\theta_r(k),\theta_r(k-1),\phi_r(k),\phi_r(k-1),\theta_s(k),\theta_s(k-1),\\ \phi_s(k),\phi_s(k-1),u_f(k),u_f(k-1),u_v(k),u_v(k-1)] \tag{5-23}$$

where the sampling interval for Eq.5-24 is 4 minutes and that for Eq.5-25 is 50 seconds respectively. The NNE consisted of two neural networks, a temperature neural network emulator and a relative humidity neural network emulator. If θ_{ri} and ϕ_{ri} are denoted as the predicted room temperature and RH respectively, the objective function is defined by

$$E_1 = \frac{1}{2}(\theta_r - \theta_{ri})^2 \tag{5-24}$$

$$E_2 = \frac{1}{2}(\phi_r - \phi_{ri})^2 \qquad (5\text{-}25)$$

In order to accelerate the training process, the input variables were normalized to the range $[-1,+1]$. The outputs of the emulator were the change in the room temperature and RH, $\Delta\theta_r$ and $\Delta\phi_r$, instead of their absolute values. Table 5-1 shows the equations used for normalization. The emulator was trained in sequential mode. The order of presentation of training examples was randomized from epoch to epoch. The training was stopped when the cost function shows no significant further reduction. The performance of the emulator was tested using another set of data that were not used in the training.

Table 5-1 Normalization function

Variable	Normalization
θ_r	$\theta_{rn} = (\theta_r - 24)/4$
ϕ_r	$\phi_{rn} = (\phi_r - 0.6)/0.2$
θ_s	$\theta_{sn} = (\theta_s - 17.5)/7.5$
ϕ_s	$\phi_{sn} = (\phi_s - 0.8)/0.2$

The air-conditioning system operated for seven days to generate input-output training pairs. Data for the first six days were used as the training set and that for the seventh day used as the validation set. The number of neurons in the hidden layer has a significant effect on the performance of the neural networks. Different numbers of nodes were investigated varying from 4 to 50. It was found that 6 neurons in the hidden layer could achieve the best performance, according to the validation result. Values of the input variable at more sampling instants, e.g. $\theta_r(k-2)$, $\theta_r(k-3)$,

$\phi_r(k-2)$, $\phi_r(k-3)$, … , were also taken as the inputs to the NNE. However, the prediction performance was not improved while more computation time was needed.

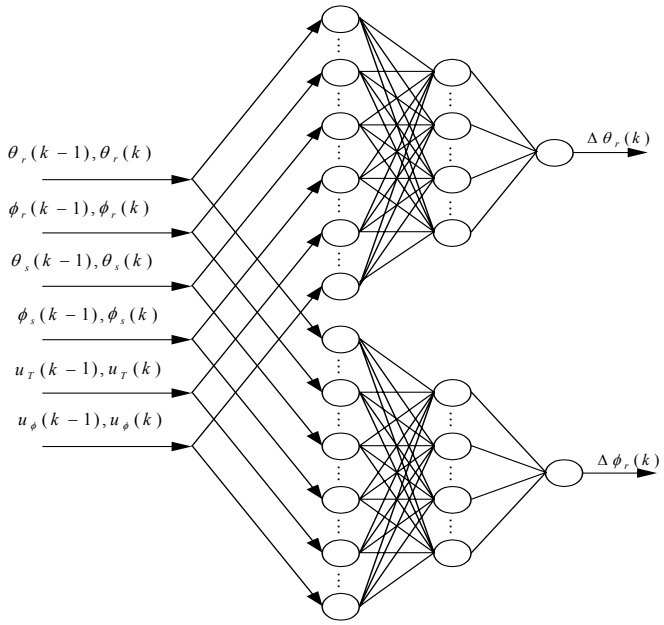

Figure 5-5 Structure of the NNE

Fig. 5-5 shows the structure of the proposed NNE consisting of two neural networks. Each neural network has 12 input nodes, 6 nodes in the hidden layer and 1 output node.

Fig. 5-6 shows the actually measured data and the predicted data using the NNE. It can clearly be noted that the predicted values for both room temperature and RH match the actual values well. In the figure, the predicted value of θ_{ri} and ϕ_{ri} were determined using

$$\theta_{ri}(k) = \theta_r(k-1) + \Delta\theta_{ri}(k) \tag{5-26}$$

$$\phi_{ri}(k) = \phi_r(k-1) + \Delta\phi_{ri}(k) \tag{5-27}$$

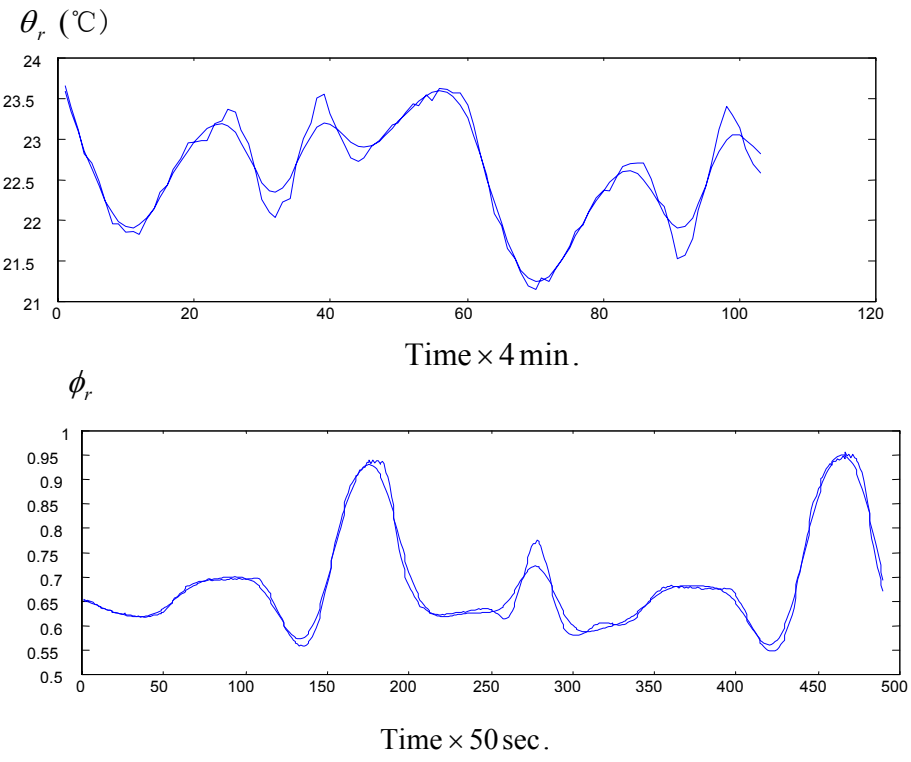

Figure 5-6 The NNE performance
(dashed line: predicted data, solid line: actual data)

5.4 Fuzzy Neural Network Controller

The FNNC was trained after the NNE has been developed.

5.4.1 Reference Response

The objective of the air-conditioning system is to keep the space at the desired condition. Before the air-conditioning plant works, the room is at a higher temperature and RH. The air-conditioning system operates to drive and maintain the two variables at their set points. Because air-conditioning is a process with a significant delay time and inertia, the transient process lasts long time. The desired system response is simply specified as the dashed line shown in Fig. 5-7.

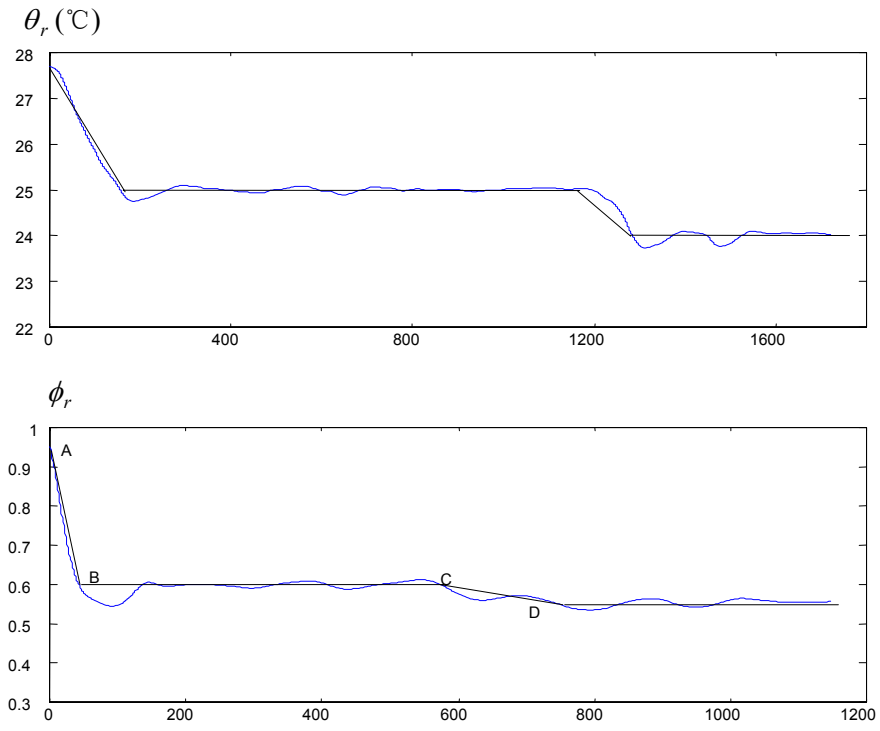

Figure 5-7 System response (dashed line: reference response, solid line: actual response)

Point A in the figure is the initial room temperature (or RH) and B represents the desired room temperature (or RH). A-B represents the system start-up. C-D represents that there is a changes in set points of the room temperature (or RH). The transient process is dependent on the property of the air-conditioning plant and the conditioned room.

5.4.2 Training of FNNC

The FNNC also consists of two fuzzy controllers, each of which is constructed like the FNN detailed in Section 5.1. These two FNNCs are trained to track the desired response of θ_r and ϕ_r. The objective function for the temperature controller is:

$$E_\theta = \frac{1}{2}(\theta_d - \theta_r)^2 \qquad (5\text{-}28)$$

The objective function for the relative humidity controller is:

$$E_{\phi} = \frac{1}{2}(\phi_d - \phi_r)^2 \tag{5-29}$$

Seven fuzzy sets, NL, NM, NS, ZO, PS, PM and PL are defined for each input variable. The same triangles as those shown in Fig. 4-3 are used in the initial definitions of the membership functions. The initial fuzzy rules are listed in Table 5-2. Because the consequent of the rules is the output increment,

$$u(k+1) = u(k)(1+y) \tag{5-30}$$

Eq.5-19 is then changed to

$$\delta^4 = \frac{-\partial E_c}{\partial y} = e_c u \frac{\partial y_p}{\partial u} \tag{5-31}$$

Table 5-2 Initial fuzzy control rules

E \ $\dot{E}$	NL	NM	NS	ZO	PS	PM	PL
NL	18	15	12	9	6	3	0
NM	15	12	9	6	3	0	-3
NS	12	9	6	3	0	-3	-6
ZO	9	6	3	0	-3	-6	-9
PS	6	3	0	-3	-6	-9	-12
PM	3	0	-3	-6	-9	-12	-15
PL	0	-3	-6	-9	-12	-15	-18

The operation of the fuzzy neural network controller is as follows. Taking the case of the room temperature, at each sampling instant, first the error term δ^4 in Eq.5-19 is computed according to the following steps:

a) With input using measured room and air supply condition, the NNE is used to predict the change in room temperature, say $\Delta\theta_r$.

b) The predicted room temperature at the (k+1)th instant is then

$$\theta_r(k+1) = \theta_r(k) + \Delta\theta_r \tag{5-32}$$

and the predicted error, e_c in Eq.5-19 is given by

$$e_c = \theta_d - \theta_r(k+1) \tag{5-33}$$

c) To determine the plant sensitivity term in Eq.5-19, the $u_f(k-1)$ and $u_f(k)$ inputs to the NNE are both increased by an amount Δ while keeping all other inputs constant. The NNE then gives a new predicted temperature change, say $\Delta\theta_r^{'}$. The plant sensitivity term is then determined as

$$\frac{\partial\theta_r}{\partial u_f} = \frac{(\Delta\theta_r^{'} - \Delta\theta_r)}{\Delta} \tag{5-34}$$

d) The term δ^4 is then computed using Eq.5-19. This error term is back-propagated through the FNNC and the connecting weights, representing the consequents of the fuzzy rules (see Chapter 4), are updated accordingly. The updated consequents are then used to generate the control action $u_f(k+1)$.

The FNNC was implemented on the air-conditioning plant with the initial fuzzy control rules as shown in Table 5-2 and initial membership functions as shown in Fig. 5-8. The actual system response is drawn by solid line in Fig. 5-7. Training of the FNNC using the desired profile as shown by the dashed line in Fig. 5-7 was done over many training cycles. It was found that initially the actual response for both temperature and RH did not follow the desired values but improved after each training cycle. After eight training cycles, the response was found to be good and the training

stopped for testing. During training, both the membership functions and the fuzzy control rules represented by connecting weights in the FNNC, change. The membership functions after eight training cycles are shown in Fig.5-9 to Fig. 5-12.

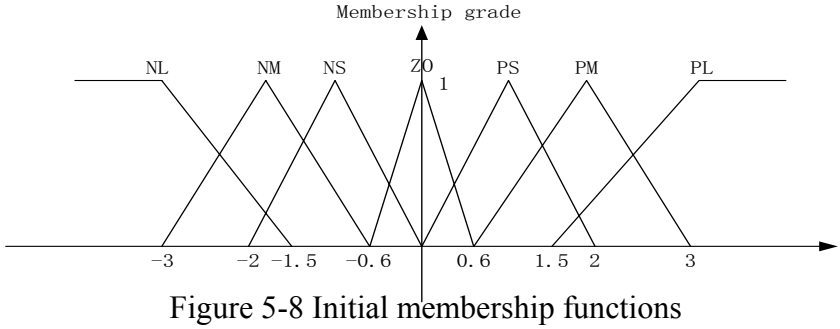

Figure 5-8 Initial membership functions

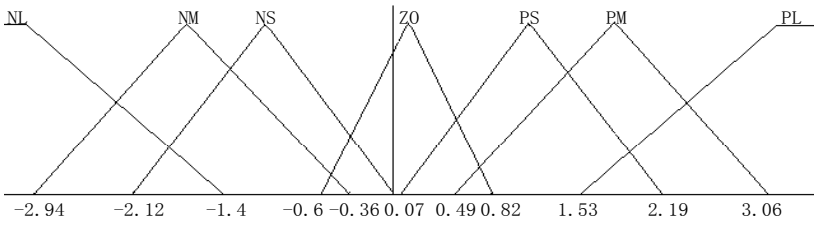

Figure 5-9 Membership functions for E_θ after training

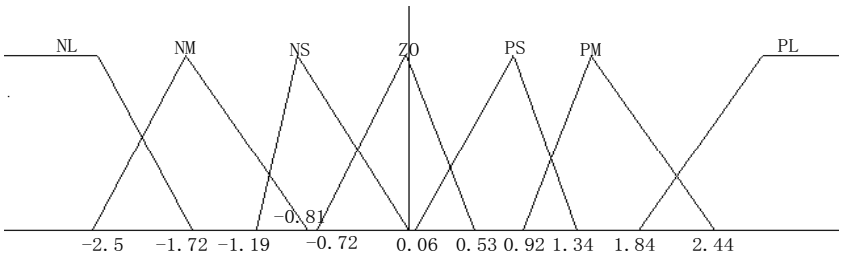

Figure 5-10 Membership functions for $\dot{E}_\theta$ after training

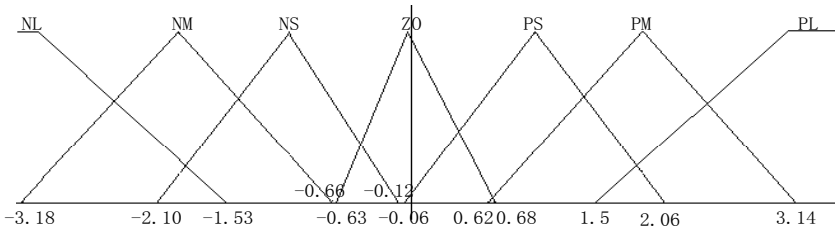

Figure 5-11 Membership functions for E_ϕ after training

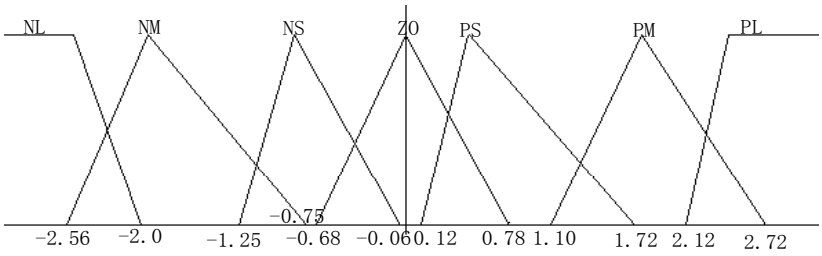

Figure 5-12 Membership function for $\dot{E}_{\phi}$ after training

The revised fuzzy rules are listed in Table 5-3 and Table 5-4.

Table 5-3 Revised control rules for temperature controller

E \ $\dot{E}$	NL	NM	NS	ZO	PS	PM	PL
NL	32	25	18	12	7	2	-5
NM	28	20	15	9	5	-1	-8
NS	22	14	8	2	-3	-6	-12
ZO	17	9	3	0	-4	-10	-18
PS	11	6	1	-3	-8	-15	-23
PM	7	2	-4	-9	-14	-22	-30
PL	2	-4	-9	-13	-19	-26	-34

Table 5-4 Revised control rules for relative humidity controller

E \ $\dot{E}$	NL	NM	NS	ZO	PS	PM	PL
NL	28	22	16	11	7	3	1
NM	22	17	13	9	5	1	-3
NS	17	12	8	3	-2	-5	-9
ZO	13	8	4	0	-3	-7	-11
PS	9	5	1	-2	-6	-11	-16
PM	4	2	-3	-8	-12	-17	-23
PL	-2	-6	-10	-14	-19	-24	-30

5.4.3 Experiment Results

After the FNNC has been trained for eight cycles, tests were performed to investigate the controller performance. Fig. 5-13 shows that the controller performed considerably

well in following the desired settings and in maintaining the room temperature and RH at their set points, 24℃ and 60% respectively. The steady state error was pretty small and oscillations were eliminated.

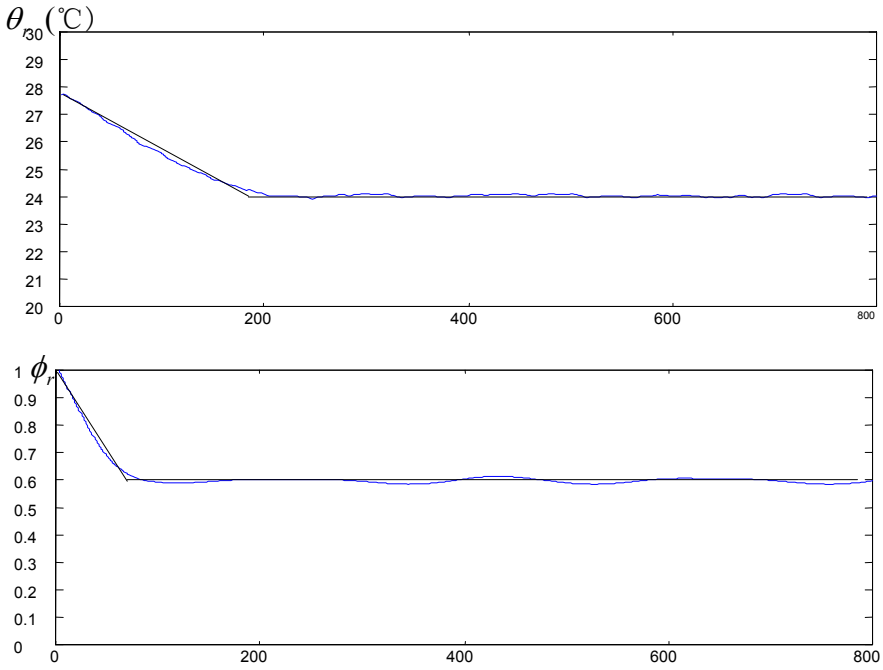

Figure 5-13 Room temperature and RH response
(dashed line: reference response, solid line: actual response)

Next, the controller's ability to track a set point change was investigated. The set point of the room temperature was changed from 24℃ to 23℃. From the response shown in Fig. 5-14, it is observed that the temperature reached and stayed at the new set point value successfully. RH remained not disturbed. Fig. 5-15 shows the response of the system when the set point for RH was changed from 60% to 50%. It can be seen that the system maintained its good response with the RH responding to the set point change accordingly while the temperature remained steady. From the two figures, it is seen that change of set point in one variable has no effect on the other variable. The controller can thus successfully deal with the coupling between variables.

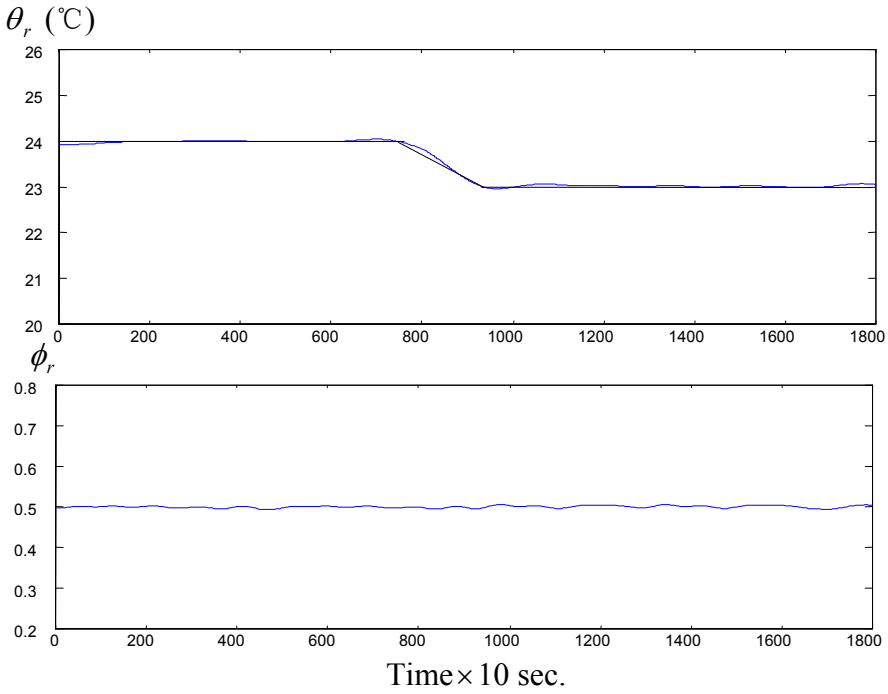

Figure 5-14 Room temperature and RH response
when set point temperature is changed
(dashed line: reference response, solid line: actual response)

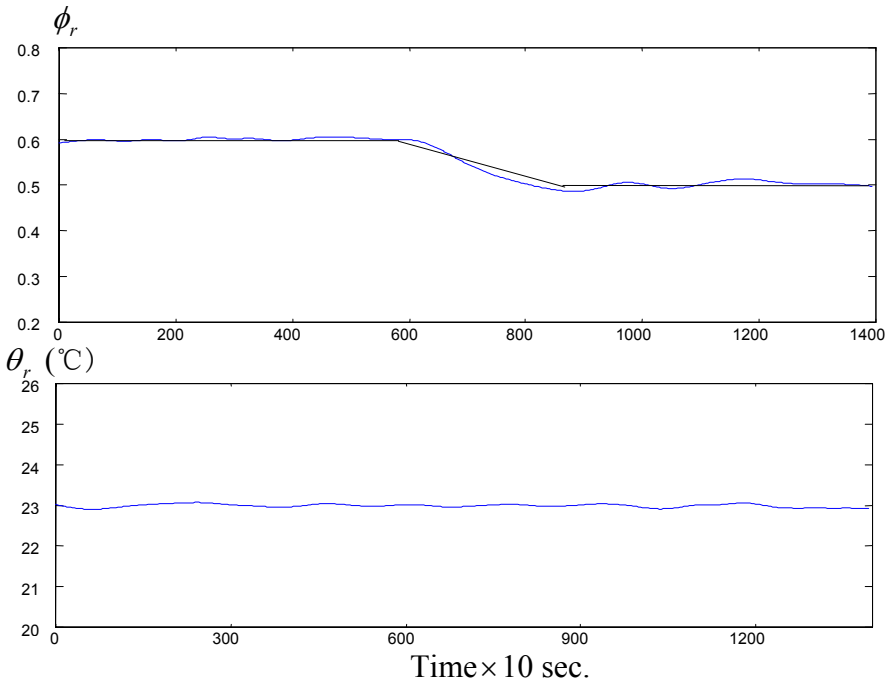

Figure 5-15 Room temperature and RH response
when set point RH is changed
(dashed line: reference response, solid line: actual response)

5.5 Concluding Remarks

The model reference adaptive control scheme was used to design the control system, in which two neural networks are constructed. A neural network emulator was devised and trained to predict the dynamics of the air-conditioning system. This emulator provided information about the system to train a fuzzy neural network controller. The system becomes the direct control if the emulator is discarded.

A three-layer perceptron was employed for the neural network emulator. The air-conditioning system was approximated as a second-order system in which the system status parameters and control actions were inputs to the emulator. The emulator was able to accurately predict both temperature and RH changes after training. The fuzzy neural network combines advantages of fuzzy logic and neural networks. The controller parameters, such as membership functions and fuzzy rules, are considered as the connecting weights in the neural network. The fuzzy controller was tuned through training of the neural network. Thus, the laborious tuning work is resolved.

From the experimental results, it was observed that the proposed control system performed very well. The fuzzy neural network controller realized self-tuning of the membership functions and fuzzy rules. The proposed control system can maintain the room temperature and RH accurately at their set points. The steady error is less than ± 0.2 ℃ and 1.5% for room temperature and relative humidity respectively. The controller also showed good set point tracking ability and was effective in decoupling temperature changes from RH changes.

CHAPTER 6
CONCLUSIONS AND RECOMMENDATIONS

This project focused on the simultaneous control of temperature and relative humidity of a conditioned space, which is required by some industrial and scientific applications, using both a fuzzy control approach and a fuzzy neural network approach. In chilled water air-conditioning systems, the cooling capacity varies with the supply airflow rate and the chilled water flow rate. A reduction in supply airflow rate or an increase in the chilled water flow rate leads to improved moisture removal. The sensible cooling capacity increases with the airflow rate and the chilled water flow rate. It is thus feasible to control space temperature and relative humidity simultaneously by varying the chilled water flow rate and the supply airflow rate.

In typical air-conditioning systems, the change in sensible and latent cooling capacity due to a percentage change in the supply air fan speed is greater than the corresponding change due to the same percentage change in the chilled water valve opening. Because the system sensible heat load and its changes are generally greater than the latent heat load and its changes, it is more logical to control space temperature by controlling the supply airflow rate and space relative humidity by controlling the chilled water flow rate. Experiments conducted on the air-conditioned space under this project also revealed the inability to control space temperature by varying water flow rate and space relative humidity by varying the supply airflow rate.

Fuzzy logic was used for the controller design in this work to resolve the difficulty of determining accurate system dynamic models. The results of the work done here show that different sampling intervals should be used for temperature and relative humidity control since their dynamic responses, in terms of system time constant, are different. The fuzzy controller used here consists of two sub-controllers, a fuzzy temperature sub-controller and a fuzzy relative humidity sub-controller. In addition to tracking the set points of room temperature and relative humidity, the fuzzy controller showed good disturbance rejection ability. The shape and distribution of the membership functions in the fuzzy controller should be chosen with care to achieve good system stability and robustness. The gains used for the input and output variables also have significant impact on the performance of the fuzzy controller and need to be chosen properly. Incorrect scaling factors can lead to system output oscillations around the set points.

Although the fuzzy controller is robust, it may not be optimal for all operating conditions. The fuzzy controller was found not to have optimum performance, and even severely degraded performance, when the membership functions or fuzzy rules are not chosen properly. Incorporating a self-tuning capability to the fuzzy controller is one way to ensure the controller always operates at its most optimal configuration. Self-learning or tuning can be achieved by integrating the fuzzy logic control with neural networks.

The model reference adaptive scheme was used to build the fuzzy neural network control system. The reference model gave the desired system output. A neural network emulator was developed to provide predictive information about the air-conditioning

system output to the fuzzy neural network controller. The fuzzy controller itself was constructed using the architecture of a neural network with the parameters of the fuzzy controller represented by connecting weights in the network. The fuzzy neural network controller is trained using actual measured plant input-output data to track the desired system output.

The neural network emulator predicted both the room temperature and the relative humidity. It was found that accurate predictions were achieved only when the temperature and the relative humidity were mapped by two separate neural networks. The neural network emulator was trained using measured plant input-output data obtained from experiments. For the emulator to perform well, the experimental training data must adequately cover the whole operating region of the system. Experiments conducted showed that accurate prediction was achieved when the air-conditioning system was approximated by a second-order dynamic model.

The fuzzy neural network provided the fuzzy logic system with the learning ability. The fuzzy neural network controller was trained after the emulator has been developed. Weights in the network were adjusted to minimize the error between the desired system output and its actual output. The fuzzy neural network controller also consisted of two sub-networks, one for temperature control and the other for relative humidity control. During system operation under control, the fuzzy neural network controller learned, using measured plant input-output data, the optimum fuzzy rules and parameters for the membership functions for fuzzy controller. In the experiments conducted, the controller successfully drove the system to follow the desired set points.

The proposed control algorithm avoided the tedious trial-and-error process in tuning of the fuzzy controller for optimum or good dynamic performance.

The proposed control strategy reduced the energy consumption because the supply air fan runs at low speeds at part load and reheat of the overcooled air was not needed. This project concentrated on the control of temperature and relative humidity. Although the proposed control strategy reduced the energy consumption, a quantitative analysis was not given. It is feasible for the power consumption to be incorporated into the objective function for training neural networks so as to achieve minimum energy operation. More studies need to be done to find the most economic way for keeping a space at set temperature and relative humidity conditions.

In this research the proposed fuzzy neural network controller successfully adjusted the membership functions and fuzzy rules. Further investigation to include self-learning of optimum scaling factors is needed because these also have significant influence on the control performance.

REFERENCE

Ahmed, O., J.W. Mitchell and S. A. Klein. Application of General Regression Neural Network (GRNN) in HVAC Process Identification and Control. ASHRAE Transaction, Vol. 102 (1), pp. 1147-1156. 1996.

Arima, M., E.H. Hara and J.D. Katzberg. A Fuzzy Logic and Rough Sets Controller for HVAC Systems. In Proc. WESCANEX 1995 Communications, Power, and Computing, Vol.1, pp. 133-138.

ASHRAE Handbook. Heating, Ventilating, and Air-Conditioning Applications. Atlanta, GA: American Society of Heating, Refrigerating and Air Conditioning Engineers. 1999.

ASHRAE Standard 55-1981. Thermal Environmental Conditions for Human Occupancy. Atlanta, GA: American Society of Heating, Refrigerating and Air Conditioning Engineers. 1981.

Astrom, K.J. and B. Wittenmark. Adaptive Control. Reading. MA: Addison-Wesley. 1989.

Beardon, C. Artificial intelligence Terminology: A Reference Guide. Ellis, Horwood. 1989.

Becker, M, D. Oestreich, H. Hasse and L. Litz. Fuzzy Control for Temperature and Humidity in Refrigeration Systems. In Proc. 1994 IEEE Conference on Control Application, Glasgow, UK, pp. 1607-1612.

Betzaida, A-S, and V-R, Miguel. Nonlinear Control of a Heating, Ventilating, and Air Conditioning System with Thermal Load Estimation. IEEE Transaction on Control System Technology, Vol. 7, No. 1, pp. 56-63. 1999.

Carlos, R. and V. Miguel. Decoupled Control of Temperature and Relative Humidity Using a Variable-Air-Volume HVAC System and Non-Interacting Control. In Proc. 2001 IEEE Conf. Control Application, Mexico City, Mexico, pp. 1147-1151.

Chen, Y. C. and C. C. Teng. A Model Reference Control Structure Using a Fuzzy Neural Network. Fuzzy Sets and Systems, Vol. 73, No. 3, pp. 291-312. 1995.

Chew A. B. Performance of Variable Air Volume Air Conditioning System. Academic Exercise, National University of Singapore. 1994.

Curtiss, P.S., J.F. Kreider and M.J. Brandemuehl. Adaptive Control of HVAC Processes Using Predictive Neural Networks. ASHRAE Transactions, Vol. 99 (1), pp. 496-504. 1993.

Curtiss, P.S., M.J. Brandemuehl and J.F. Kreider. Energy Management in Central HVAC Plants Using Neural Networks. ASHRAE Transaction, Vol. 100 (1), pp. 476-493. 1994.

Curtiss, P. S. Experimental Results from a Network-Assisted PID Controller. ASHRAE Transaction, Vol. 102 (1), pp. 1157-1168. 1996.

Cybenko, G. Approximation by Superposition of a Sigmoidal Function. Mathematics of Control, Signals, and Systems, 2(4), pp.303-314. 1989.

Ding, Y. and K.V. Wong. Control of Simulated Dual-Temperature Hydronic System Using a Neural Network Approach. ASHRAE Transaction, Vol.96, pp.727-732. 1990.

Funakoshi, S. and K. Matsuo. PMV-Based Train Air-Conditioning Control System. ASHRAE Transactions, Vol. 101 (1), pp.423-430. 1995.

Haykin, S. Neural Networks: A Comprehensive Foundation (2nd ed.). Upper Saddle River: Prentice Hall, 1999.

He, X., S. Liu, H. Harry and H. Itoh. Multivariable Control of Vapor Compression Systems. HVAC&Research, Vol. 4, No. 3, pp. 205-230. 1998.

Huang, S. and R.M. Nelson. A PID-Law-Combining Fuzzy Controller for HVAC Applications. ASHRAE Transactions, Vol. 97 (2), pp. 768-774. 1991.

Huang, S. and R.M. Nelson. Delay Time Determination Using an Artificial Neural Network. ASHRAE Transactions, Vol. 100 (1), pp. 831-840. 1994.

Huang, S. and R.M. Nelson. Rule Development and Adjustment Strategies of a Fuzzy Logic Controller for an HVAC System: Part One-Analysis. ASHRAE Transactions, Vol. 100(1), pp. 841-850. 1994.

Huang, S. and R.M. Nelson. Rule Development and Adjustment Strategies of a Fuzzy Logic Controller for an HVAC System: Part Two-Experiment. ASHRAE Transactions, Vol. 100(1), pp. 851-856. 1994.

Huang, S. and R.M. Nelson. Development of a Self-Tuning Fuzzy Logic Controller. ASHRAE Transactions, Vol. 105 (1), pp. 206-213. 1999.

Ibrahim, R. Opportunities to Improve Energy Efficiency. IES Seminar on Energy Savings, Clean Technology & Tax Incentives. Feb. 1998.

Jang, J-S. R. ANFIS: Adaptive-Network-Based Fuzzy Inference System. IEEE Transactions on Systems, Man and Cybernetics, Vol. 23, No. 3. pp. 665-685. 1993.

Jones, W. P. Air Conditioning Engineering (4th ed.). London: Edward Arnold. 1994.

Kasahara, M., T. Matsuba, Y. Kuzuu, T. Yamazki, Y. Hashimoto, K. Kamimura and S. Kurosu. Design and Tuning of Robust PID Controller for HVAC Systems. ASHRAE Transactions, Vol. 105 (2), pp. 154-166. 1999.

Kasahara, M., Y. Kuzuu, T. Matsuba, Y. Hashimoto, K. kamimura and S. Kurosu. Physical Model of an Air-Conditioned Space for Control Analysis. ASHRAE Transactions, Vol. 106 (2), pp. 304-317. 2000.

Kasahara, M., T. Yamazaki, Y. Kuzuu, Y. Hashimoto, K. Kamimura, T. Matsuba and S. Kurosu. Stability Analysis and Tuning of PID Controller in VAV Systems. ASHRAE Transaction, Vol.107 (1), pp. 285-296. 2001.

Khalid, M., S. Omatu and R.Yusof. Temperature Regulation with Neural Networks and Alternative Control Schemes. IEEE Transaction on Neural Networks, Vol. 6, No. 3, pp. 572-582. 1995.

Khattar, M.K and H.I. Henderson. Impact of HVAC Control Improvements on Supermarket Humidity Levels. ASHRAE Transactions, Vol. 105 (1), pp. 521-532. 1999.

Kolmogorov, A.N. On the Representation of Continuous Functions of Many Variables by Superposition of Continuous Functions of One Variable and Addition. Doklady Akademii Nauk SSR, Vol. 114. pp. 953-956. 1957. English translation. Mathematical Society Transaction, Vol. 28. pp. 55-59. 1963.

Krakow, K.I., S. Lin. and Z. Zeng. Temperature and Humidity Control During Cooling and Humidifying by Compressor and Evaporator Fan Speed Variation. ASHRAE Transactions, Vol. 101, pp. 292-304. 1995a.

Krakow, K.I., S. Lin. and Z. Zeng. Analytical Determination of PID Coefficients for Temperature and Humidity Control During Cooling and Dehumidifying by Compressor and Evaporator Fan Speed Variation. ASHRAE Transactions, Vol. 101, pp. 343-354. 1995b.

Liu, M., Y. Zhu and B.Y. Park. Airflow Reduction to Improve Building Comfort and Reduce Building Energy Consumption-A Case Study. ASHRAE Transactions, Vol. 105 (1), pp. 384-394. 1999.

Ljung, L. System Identification: Theory for the User (2nd ed.). Upper Saddle River, N.J.: Prentice Hall, 1999.

Luxton, R.E. and A. Shaw. Process Within a Dehumidifier Coil and Their Consequences in Air-Conditioning Design. 3rd ASME-JSME Thermal Engineering Joint Conference, March 1991. Reno, Nevada.

Matsuba, T., M. Kasahara, I. Murasawa, Y. Hashimoto, K. Kamimura, A. Kimbara and S.Kurosu. Stability Limit of Room Air Temperature of a VAV System. ASHRAE Transaction, Vol. 104 (2), pp. 257-265. 1998.

Medsker, L.R. Hybrid Intelligent Systems. Norwell, Mass.: Kluwer Academic Publishers, 1995.

Narendra, K.S. and K. Parthasarathy. Identification and Control of Dynamical Systems Using Neural Networks. IEEE Transactions on Neural Networks, Vol. 1, No. 1, pp. 4-27. 1990.

Narendra, K.S., R. Ortega and P. Dorato. Advances in Adaptive Control. New York: IEEE Press. 1991.

Nørgaard, M., O. Ravn, N.K. Poulsen and L.K. Hansen. Neural Networks for Modeling and Control of Dynamic Systems: a Practitioner's Handbook. New York: Springer. 2000.

Parker, D.S., J.R. Sherwin, R.A. Raustad and D.B.Shirey. Impact of Evaporator Coil Airflow in Residential Air-Conditioning Systems. ASHRAE Transactions, Vol. 103 (2), pp. 395-405. 1997.

Pedrycz, W., Fuzzy Control and Fuzzy Systems. N.Y.: John Wiley & Sons, 1989.

Rosandich, R. Understanding Controllers and Control Terminology. ASHRAE Journal, Vol. 39, No. 9, pp. 22-25. 1997.

Shaw, I.S. Fuzzy Control of Industrial Systems: Theory and Applications. Norwell, Mass.: Kluwer Academic Publishers, 1998.

Shirey, D.B. Demonstration of Efficient Humidity Control Techniques at an Art Museum. ASHRAE Transactions, Vol. 99 (1), pp. 694-703. 1993.

So, A. T. P., T. T. Chow, W. L. Chan and W. L. Tse. Fuzzy Air Handling System Controller. Building Services Engineering Research and Technology, Vol. 15, No. 2, pp. 95-105. 1994.

So, A.T.P., T.T. Chow, W.L. Chan and W.L. Tse. A Neural-Network-Based Identifier/Controller for Modern HVAC Control. ASHRAE Transactions, Vol. 101 (2), pp. 14-31. 1995.

So, A. T. P., W. L. Chan and W. L. Tse. Self-Learning Fuzzy Air Handling System Controller. Building Services Engineering Research and Technology, Vol.18, No. 2, pp. 99-108. 1997.

Sugeno, M., Industrial Applications of Fuzzy Controller. Elsevier Science. 1985

Underwood, C.P. HVAC Control Systems: Modeling, Analysis and Design. pp.78-115, E & FN SPON. 1999.

Xi, W. Y., A.N. Poo and M. Ang. On the Generation of Suitable Data Sets for the Off-Line Training of Neural-Network Controllers Using Actual Plant Data. International Symposium of Intelligent Automation and Control, May 1998, Alaska, USA.

Zhu Y.C. Multivariable System Identification for Process Control. New York: Pergamon.2001.

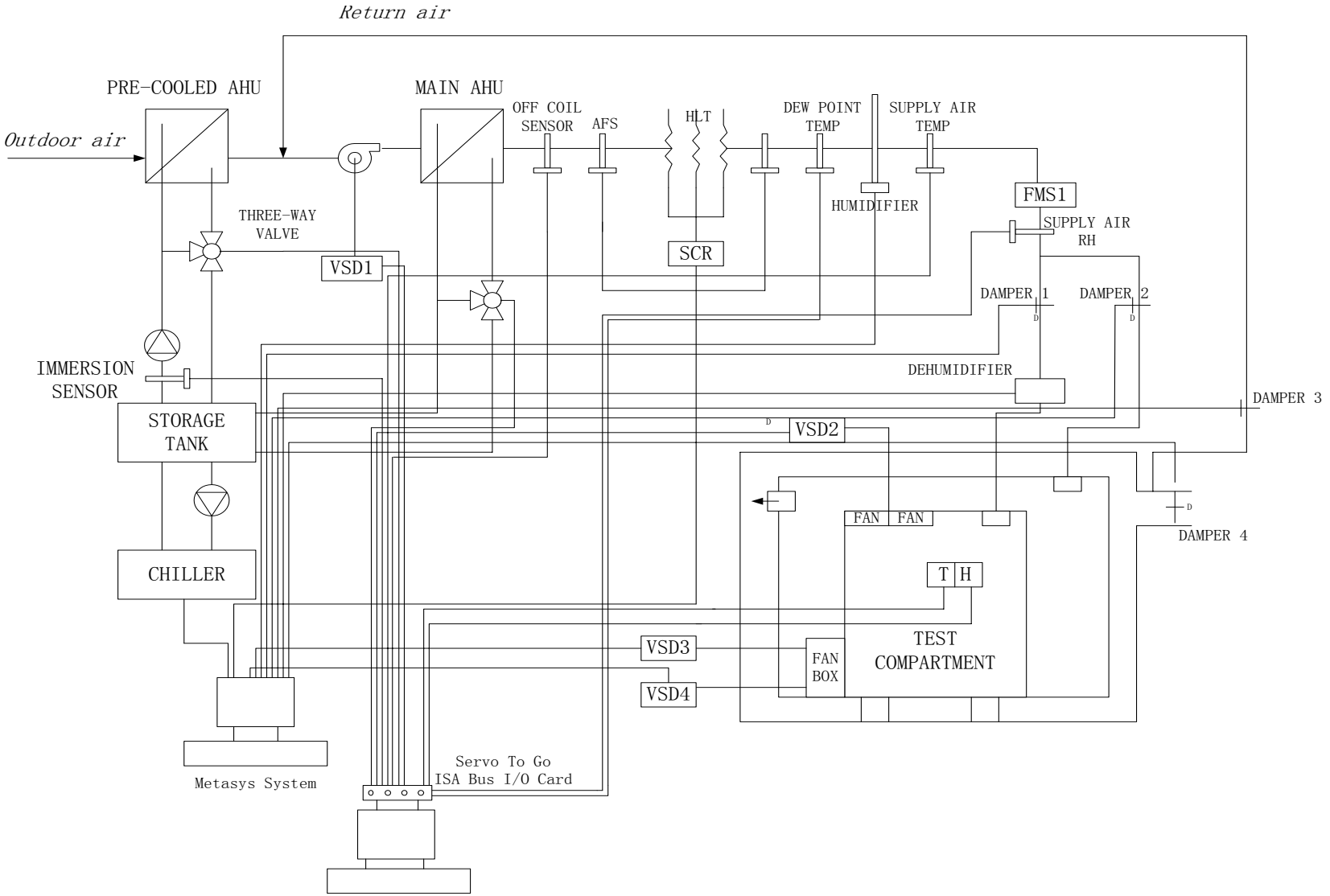
Return air
PRE-COOLED AHU
MAIN AHU
Outdoor air
OFF COIL SENSOR
AFS
HLT
DEW POINT TEMP
SUPPLY AIR TEMP
HUMIDIFIER
FMS1
SUPPLY AIR RH
THREE-WAY VALVE
VSD1
SCR
DAMPER 1
DAMPER 2
IMMERSION SENSOR
DEHUMIDIFIER
DAMPER 3
STORAGE TANK
VSD2
FAN
FAN
DAMPER 4
CHILLER
T
H
TEST COMPARTMENT
VSD3
FAN BOX
VSD4
Servo To Go ISA Bus I/O Card
Metasys System